Ultracentrifuge Studies with Rayleigh Interference Optics. II. Low-Speed Sedimentation Equilibrium of Homogeneous Systems*

E. G. Richards, D. C. Teller,† and H. K. Schachman

ABSTRACT: Procedures are presented for the determination of molecular weights by the low-speed sedimentation equilibrium method coupled with a synthetic boundary experiment which is used for the labeling of the Rayleigh interference fringes. Emphasis is placed on experimental details concerning the planning and performance of the experiments and also on the reading of interference patterns. A method is described for determination of the optimum rotor velocity leading to resolvable fringes at the bottom of the cell for solutions of varying concentrations and column heights. General equations are used which permit the calculation of both weight and z-average molecular weights for polydisperse, ideal systems, as well as the molecular weight and second virial coefficient for two-component, nonideal systems. Labeling of fringes is accomplished by both conservation of mass in the cell and by location of the hinge point with the aid of the white-light fringe. Agreement of results by the two methods generates confidence that (1) all material in the cell was accounted for, (2) the fringe labeling was correct, and (3) no calculation errors were made. To eliminate tedious calculations necessary for thorough evaluation of the available data on the interference patterns, a computer program was developed to handle both conservation of mass and white-light fringe labeling. This program was found to be reliable upon testing with simulated data obtained from another program. Since the accuracy of this method depends upon the value for the initial concentration of the solute as determined from the synthetic boundary experiment, its reliability was checked and found to be accurate to ± 0.02 fringe or better for sucrose solutions in a concentration range of 1–4 g/dl. Sedimentation equilibrium experiments performed with the same solutions gave a molecular weight extrapolated to zero concentration accurate to about 0.5%, and a second virial coefficient in good agreement with data obtained from isopiestic data. Results obtained for a sample of ribonuclease at concentrations from 0.2 to 0.7 g/dl gave molecular weights with a precision of about 0.5%. The average value of 13,170, although slightly lower than that based on the known structure of RNase, was used to illustrate some of the potential sources of error that exist in the sedimentation equilibrium technique. Finally, a simple overspeeding procedure is described which permits a considerable reduction (about two-thirds) in the time required to reach sedimentation equilibrium.

Despite the long-standing and sound theoretical foundation of the sedimentation equilibrium method (Svedberg, 1925; Svedberg and Pedersen, 1940), until recently it was used only rarely for the determination of molecular weights of large and small molecules. The resurgence of the method in the past 6 years stems principally from the large reduction in the time required for an experiment and the greatly increased accuracy in the optical registration of concentration distributions. It had been known since 1924 that the time required to attain sedimentation equilibrium depended essentially on the square of the height of the liquid column (Mason and Weaver, 1924). However, this knowledge was rarely used until 1958, when Van Holde and Baldwin extended this theoretical treatment and demonstrated experimentally that accurate molecular weights could be obtained in experiments of short duration through the use of short liquid columns. The sedimentation equilibrium technique received an additional stimulus from the adaptation to the ultracentrifuge of various interference optical systems (Beams *et al.*, 1954; Richards and Schachman, 1959). The incorporation of interferometry led to a substantial increase in the accuracy of measuring the concentration distribution while at the same time provided for automatic corrections for cell window distortions and for refractive index changes stemming from pressure effects and redistribution of buffer salts and other small molecules present in the solvent.

As a consequence of the renewed interest in the sedimentation equilibrium method many extensions to the theory have resulted (Fujita, 1962; Osterhoudt and Williams, 1965; Fujita and Williams, 1966; Don-

* From the Department of Biochemistry and Virus Laboratory (H. K. S.) and the Department of Nutritional Sciences, Institute of Marine Resources (E. G. R.), University of California, Berkeley, California 94720; and the Department of Biochemistry, University of Washington School of Medicine, Seattle, Washington 98105 (D. C. T). *Received August 3, 1967.* This investigation was supported in part by Public Health Service Research Grants GM 09899, GM 13401, and GM 12159 from the National Institute of General Medical Sciences, U. S. Public Health Service, by a National Science Foundation research grant (GM 4810X), and by a contract between the Office of Naval Research and the Regents of the University of California.

† Taken in part from a thesis submitted by D. C. T. in partial satisfaction of the requirements for the Doctor of Philosophy degree, Department of Biochemistry, University of California, 1965.

nelly, 1966). The theory for calculation of the time required to reach equilibrium (Mason and Weaver, 1924; Van Holde and Baldwin, 1958) has been extended to cover the time required to reach a new equilibrium distribution after a change of speed (Klenin *et al.*, 1966) and also the time required to reach equilibrium for a slowly decelerating rotor (Billick *et al.*, 1966).

Even though Rayleigh interferograms provide directly and simply an accurate measure of the concentration difference between any two positions in the cell, absolute concentrations are not deduced readily. Methods are required, therefore, for the determination of the absolute concentration (in fringes) at any specific position such as the meniscus. With this information values of the concentration at other positions are calculated easily. One of the first methods for evaluating concentrations made use of a synthetic boundary cell to measure the initial concentration coupled with the location of the white-light fringe or a treatment based on the conservation of mass of material in the sector-shaped ultracentrifuge cell (Ginsburg *et al.*, 1956; Richards and Schachman, 1959). Subsequently several procedures have been proposed to eliminate the need for the separate synthetic boundary experiment. The most promising of these has been the method of Yphantis (1964), in which a solution at relatively low concentration is centrifuged at a speed sufficiently high that the concentration at the meniscus is reduced essentially to zero. Osterhoudt and Williams (1965) noted that data obtained with the same cell at equilibrium at different speeds are sufficient to obtain the molecular weight. LaBar (1965) developed an alternative method in which the speed was increased after equilibrium was achieved. Through this means, a zero concentration reference near the meniscus was provided. The use of both the Rayleigh and schlieren optical systems simultaneously has been shown to provide a molecular weight for homogeneous materials (Chervenka, 1966).

In spite of the success of the high-speed method of Yphantis (1964) there are systems for which low-speed sedimentation equilibrium experiments are desirable. The high-speed experiment is not well suited for samples containing contaminants of low molecular weight; sometimes it is difficult to account for all the material in the cell. Trimers, tetramers and higher polymers, if present, may escape detection. Since the high-speed method is limited to dilute solutions, it is not suitable when results at higher concentrations are required, as for some interacting systems. Finally, the low-speed experiment, at the present time, is capable of yielding results of greater accuracy for the determination of weight- and z-average molecular weights.

This paper presents procedures utilized for the determination of both the weight- and z-average molecular weights by the conventional low-speed sedimentation equilibrium method which requires the additional synthetic boundary experiment for labeling the fringes on an absolute scale. A computer program was developed to exploit as fully as possible the data available on the photographic plate. This permitted an increase in accuracy and reliability by providing a comparison between results obtained from the conservation of mass and those from the white-light fringe method.

Since sedimentation equilibrium experiments, even with short columns, require times of the order of 12–18 hr, or greater, efforts were devoted to devise a technique which would permit a substantial reduction in this time. The procedure presented herein leads to a shortening in the duration of the experiment comparable to that achieved by the procedure of Hexner *et al.* (1961). Emphasis was directed in the present work on practical rather than theoretical aspects.

Theoretical

Sedimentation Equilibrium Equations. Although the basic theory of sedimentation equilibrium can be written in many alternative forms (Williams *et al.*, 1958; Van Holde and Baldwin, 1958; Fujita, 1962), the following equations were employed since they are suitable for ideal and nonideal two-component solutions, as well as for ideal polydisperse solutions. The following discussion is directed to two-component systems but the terminology for the apparent weight and z-average molecular weights, M_w^{app} and M_z^{app}, was selected since the equations are applicable to ideal, polydisperse systems. The second and third virial coefficients are included for the sake of completeness; for many systems they are so small that the molecular weight dependence on concentration is negligible. In some cases considered here $1/M^{app}$ varies linearly with concentration.

For a two-component, nonelectrolyte system at equilibrium the concentration c of solute as a function of distance in the cell can be written (Fujita, 1962)

$$2MArc = [1 + (B_1M + \bar{V})c + (2B_2M^2 + B_1M\bar{V} + \bar{V}_1^2)c^2 + \ldots]\frac{dc}{dr} \quad (1)$$

$$A = \frac{(1 - \bar{V}\rho_0)\omega^2}{2RT} \quad (1a)$$

where M is the molecular weight and $\bar{V}$ is the partial specific volume of the solute, ρ_0 is the density of the solvent, ω is the angular velocity, r is the distance from the center of rotation, and R and T are the gas constant and the absolute temperature. It should be noted that the density term (ρ_0) in eq 1a corresponds to the pure solvent. Thermodynamic theory leads, of course, to the density of the solution (Goldberg, 1953), but eq 1 includes the relationship between the densities of the solvent and solution in terms of the concentration of the redistributing solute. The coefficients B_1 and B_2 are obtained from the expansion relating the activity coefficient (y) of the solute to its concentration (c) measured in grams per milliliter.

$$\ln y = MB_1c + M^2B_2c^2 + \ldots \quad (2)$$

Equation 1 has been integrated by Fujita (1962)

for a sector-shaped cell to give

$$\frac{1}{M_w^{app}} = \frac{1}{M} + B_1^* \frac{(c_m + c_b)}{2} + \frac{2B_2^* M}{3}(c_b^2 + c_b c_m + c_m^2) + \ldots \quad (3)$$

where M_w^{app} is an apparent molecular weight[1] defined by

$$M_w^{app} = \frac{c_b - c_m}{A(r_b^2 - r_m^2)c_0} \quad (4)$$

and B_1^* and B_2^* are

$$B_1^* = B_1 + \frac{\bar{V}}{M}$$

$$B_2^* = B_2 + \frac{\bar{V}B_1}{2M} + \frac{\bar{V}^2}{2M^2} \quad (5)$$

The subscripts m and b refer to quantities evaluated at the top (meniscus) and the bottom of the liquid column and c_0 is the initial concentration of solute.

Equation 1 may also be arranged in a manner that is appropriate for plots of ln c *vs.* r^2. For a two-component system composed of solvent and solute

$$1/M_{w,r}^{app} = \frac{1}{M} + B_1^* c + 2B_2^* M c^2 + \ldots \quad (6)$$

where $M_{w,r}^{app}$ is an apparent molecular weight evaluated at any level r and defined by

$$M_{w,r}^{app} = \frac{1}{A}\frac{d \ln c}{dr^2} \quad (7)$$

This equation is used for evaluating the apparent molecular weight at r_m and r_b. It has been shown by Van Holde and Baldwin (1958) that, for a nonideal, two-component system, the apparent molecular weight calculated from eq 4 corresponds to the concentration $(c_m + c_b)/2$. Thus it is of interest to compare with M_w^{app} the apparent molecular weight $M_{w,\bar{c}}^{app}$ obtained from eq 7 at the same concentration, since the former involves an extrapolation procedure potentially less accurate than the interpolation necessary for the latter.

Finally eq 7 may be written for the top and bottom of the liquid column and the resulting expressions introduced into the relationship (Lansing and Kraemer, 1935)

$$M_z^{app} = \frac{c_b M_{w,b}^{app} - c_m M_{w,m}^{app}}{c_b - c_m} \quad (8)$$

to give

$$\frac{1}{M_z^{app}} = \frac{1}{M} + B_1^*(c_b + c_m) + 2MB_2^*(c_b^2 + c_b c_m + c_m^2) + MB_1^{*2} c_b c_m + \ldots \quad (9)$$

For an ideal, polydisperse system with all species having the same partial specific volume, eq 4 and 8 give, respectively, the weight- and z-average molecular weights.

Calculation of Appropriate Rotor Speed. In the equations derived below, the dependent variable, c_b/c_m or ln (c_b/c_m), at equilibrium is employed rather than the more common $1/\ln (c_b/c_m)$. This preference is based upon the fact that for low-speed equilibrium experiments, c_b/c_m lies between 1 and 10; this range is more convenient than the ∞ to 0.434 for $1/\ln (c_b/c_m)$.

Since accuracy in the molecular weight measurement is increased by having a large value for $c_b - c_m$, the rotor velocity should be as high as possible consistent with other experimental restrictions. If the velocity is too large, the concentration gradient at the cell bottom may be sufficiently high that the light is deviated so much that it cannot traverse the optical system without being intercepted by lens holders or other opaque components in the optical path. Even at slightly lower velocities the gradient may be so steep that the fringes cannot be resolved. To select the maximum speed which will still give a measurable separation of fringes at the bottom of the solution, it is necessary to determine $(dc/dr)_b$ in terms of parameters which can be readily evaluated.

In order to simplify the derivations which follow, a two-component, ideal solution is considered; hence the correction terms containing the activity coefficient and $\bar{V}$ may be neglected. For ease of computation, the equations are expressed as a function of c_b/c_m at equilibrium. An integrated from of eq 1 (seen here as eq 10)

$$M = \frac{\ln \frac{c_b}{c_m}}{A(r_b^2 - r_m^2)} \quad (10)$$

can be combined with eq 1 written for the bottom of the cell to give

$$\frac{c_b}{c_0} \ln \frac{c_b}{c_m} = \frac{(r_b^2 - r_m^2)(dc/dr)_b}{2c_0 r_b} \quad (11)$$

The term c_b/c_0 can be obtained by combination of eq 4 and 10. Equations 10–12 (Richards, 1960) are used

$$\frac{c_b}{c_0} = \frac{\frac{c_b}{c_m} \ln \frac{c_b}{c_m}}{\frac{c_b}{c_m} - 1} \quad (12)$$

to determine the equilibrium speed as described in the Experimental Section.

[1] In the derivation of eq 3, Fujita considered only a two-component system consisting of a homogeneous solute and solvent. For such systems, the left-hand side of the equation is $1/M^{app}$, where M^{app} is the apparent molecular weight, *i.e.*, uncorrected for effects due to the nonideality of the solution. The treatment presented here (see eq 7) allows for polydispersity and thus $1/M^{app}$ is written as $1/M_w^{app}$ in eq 3 even though that equation is written for a two-component system.

Procedure for Reducing Time Required for Attainment of Sedimentation Equilibrium. The principal drawback to the sedimentation equilibrium method lies in the considerable time required to attain the equilibrium distribution (Mason and Weaver, 1924; Van Holde and Baldwin, 1958). This time can be reduced substantially by first overspeeding the rotor for a brief period and then lowering the centrifugal field to that desired (Richards and Schachman, 1959; Richards, 1960; Hexner *et al.*, 1961). This overspeeding procedure leads rapidly to a concentration distribution which closely approximates that obtained much more slowly at the lower (desired) speed. To estimate the overspeeding velocity and time at that speed Hexner *et al.* (1961) used a theoretical approach based on the treatment of Mason and Weaver (1924). An alternative approach is described here.

In any sedimentation equilibrium experiment a certain amount of solute must be accumulated between the "hinge point" (r_0) (that level in the solution column where the concentration at equilibrium is equal to the initial concentration) and cell bottom. The accumulated material (m_a) (for the desired equilibrium speed (ω)) may be determined from the expression

$$m_a = \phi \int_{r_0}^{r_b} (c - c_0) r dr \qquad (13)$$

where ϕ is the product of the sectorial angle and the cell thickness along the direction of the optical path and c is the concentration at any level (at equilibrium). The overspeeding procedure must be so designed as to allow for a rapid transport of the correct amount of solute past the hinge point. The material m_s transported across the surface at r_0 in the plateau region is given by the relationship (Svedberg and Pedersen, 1940; Schachman, 1959)

$$m_s = \phi \omega'^2 r_0^2 s c_0 \int_0^{t'} e^{-\omega'^2 s t} dt \qquad (14)$$

where t' is the time of overspeeding at the higher angular velocity (ω') and s is the sedimentation coefficient *under the experimental conditions.* The value of t' for a given ω' is determined by equating m_s to m_a. Upon substituting an integrated form of eq 1 (the concentration-dependent terms within the brackets being neglected)

$$c = c_0 e^{MA(r^2 - r_0^2)} \qquad (15)$$

and integrating the resulting expression, we obtain

$$r_0^2(1 - e^{-2\omega'^2 s t'}) = \frac{1}{MA}[e^{MA(r_b^2 - r_0^2)} - 1] - (r_b^2 - r_0^2) \qquad (16)$$

Equation 16 expresses the equality between the mass transported by sedimentation at ω' and the mass accumulated between the surface at r_0 and the cell bottom after sedimentation equilibrium has been achieved.

The exponential term on the left side of eq 16 can be expanded in a Taylor's series with only two terms retained since $\omega'^2 s t' \ll 1$. Further simplification is achieved by the substitution of eq 15 written for the bottom of the cell.

$$2\omega'^2 s t' = \frac{c_b/c_0 - 1 - \ln (c_b/c_0)}{MAr_b^2 - \ln (c_b/c_0)} \qquad (17)$$

It should be pointed out that this equation underestimates the time required to transport the necessary material m_a when the plateau disappears during the overspeeding period. The use of eq 17 to calculate the overspeeding period is described in the Experimental Section.

Location of Hinge Point. It is advantageous to know the approximate location of the hinge point for a given set of conditions. This position is readily evaluated by combining eq 10 with the logarithmic form of eq 15 written for the bottom of the cell; this leads to

$$r_0^2 = r_b^2 - (r_b^2 - r_m^2) \frac{\ln \frac{c_b}{c_0}}{\ln \frac{c_b}{c_m}} \qquad (18a)$$

An alternate expression, useful for obtaining the fractional position of the hinge point from the bottom of the solution, can be obtained by factoring the above equation.

$$\frac{r_b - r_0}{r_b - r_m} = \frac{r_b + r_m}{r_b + r_0} \frac{\ln (c_b/c_0)}{\ln (c_b/c_m)} \qquad (18b)$$

Since the ratio $(r_b + r_m)/(r_b + r_0)$ is close to unity, the hinge point is determined readily by successive approximation.

Experimental Section

Materials. Sucrose was obtained from Mallinckrodt Chemical Works. RNase chromatographically prepared but not freeze dried (code no. RAS6081) was purchased from Worthington Biochemicals Corp. Sucrose solutions of known concentration were prepared gravimetrically, with correction made for the buoyancy of air. Dilutions of stock solutions were also made gravimetrically. After preparation the solutions were stored on ice in a refrigerator. To increase the refractive index of the reference liquid (Richards and Schachman, 1959), 1,3-butanediol, obtained from Eastman Organic Chemicals, was used directly from the bottle. Fluorochemical FC-43 (Yphantis, 1960) was used to provide an inert, transparent liquid (Ginsburg *et al.*, 1956) beneath the solution columns in the ultracentrifuge cells.

Ultracentrifuge. The experiments were performed with a Spinco Model E ultracentrifuge equipped with a temperature control system and the Svensson modification of the Rayleigh interferometer (Svensson, 1950; Richards and Schachman, 1959). The optical system was aligned according to the procedure of E. G. Richards, R. H. Haschemeyer, D. Teller, and H. K. Schachman (in preparation); the camera lens was focused half-way through the cell. The experiments involving the molecular weights of RNase and sucrose were performed in a machine equipped with adjustable optical components (Gropper, 1964), including the light source mount, mask holder, mirror mount, camera lens mount, and cylindrical lens mount. For the experiments in which the time to equilibrium was measured, other adjustable optical components (light-source mount, interference mask holder, and cylindrical lens mount) (Richards and Schachman, 1959) were used. A symmetrical aperture with slits 0.44 mm wide was used. To isolate the mercury line at 546 mμ, a Bausch and Lomb second-order interference filter was sandwiched with a Wratten No. 15 filter (which blocks transmission at 373 mμ) to give a combined thickness of $^3/_8$ in. Recent work, including the equilibrium experiments reported below, was performed with a Baird–Atomic B-9 interference filter of $^3/_8$-in. thickness. This filter, which passes twice the light at 546 mμ with one-half the band width, allows a concentration difference corresponding to 120 fringes to be measured. The spectrum of the filters was measured using a Cary 15 recording spectrophotometer. Either aluminum-filled or clear epon double-sector centerpieces were used. Reproducible filling of cells was facilitated by the use of Hamilton syringes with Cheney adapters. Photographs were taken on Kodak spectrographic plates, type II-G. The patterns were read using either a Gaertner M2001-P ultracentrifuge comparator or a Nikon Shadowgraph Model 6C equipped with a 50× objective lens and zero-adjusting collars. The thickness of the double-sector centerpieces in the direction of the optical path was measured with the aid of an appropriate micrometer on tightened cells assembled with drilled-out window holders.

Synthetic Boundary Experiment. Prior to the equilibrium experiment the value for c_0 was determined with a double-sector synthetic boundary cell. With materials of sufficiently high molecular weight, the solution was dialyzed against the solvent; materials of low molecular weight were dissolved directly in the solvent. To minimize the possibility of evaporation, which could have led to an erroneous value for c_0, certain precautions were taken: (1) the centrifugation was performed soon after removal of the solution from the dialysis sac; (2) small volumes were not allowed to stand in large containers; (3) all manipulations, including filling of cells, were performed in a cold room; and (4) solutions were stored in covered tubes placed on ice.

In the right-hand compartment (screw ring facing the worker) of an interference cell assembled with a double-sector, synthetic boundary centerpiece was placed 0.14 ml of solution and in the other 0.44 ml of solvent (for problems associated with volumes employed in the synthetic boundary cell, see LaBar, 1966). The placement of the solution in the right-hand compartment was dictated by the desire to have the fringes curve upwards with an increase in distance from the axis of rotation. To permit temperature equilibration of the cell and rotor, a period of 5–10 min was allowed to pass before evacuating the chamber. Since the specific refractive increment varies with temperature, synthetic boundary and equilibrium experiments were performed at the same temperature. As soon as the evacuation of the chamber was started, the rotor was accelerated at 6 amp until the boundary formed and then at 10 amp until the menisci were superimposed. (This occurred before 20,000 rpm.) At this time an interference pattern was obtained, and another when the fringes in the boundary region were resolvable in the viewing screen. For rapidly sedimenting materials, the speed of the rotor was immediately reduced on medium or fast brake and diffusion allowed to occur at about 5000 rpm. (Above this speed we have not observed convective disturbances during braking.) At the conclusion of the centrifugation the rotor was removed from the chamber and shaken (without removing the cell or disturbing its orientation in the rotor) in order to destroy the concentration gradient; then the rotor was returned to the operating speed and the base-line picture taken.

After destruction of the gradient, the density of the liquid in the solution compartment above the channel increases; consequently solution is forced into the solvent limb until the hydrostatic pressure is the same at the level of the channel. Since the solution that flows into the reference compartment is of greater density than the solvent, it flows to the bottom with the result that a concentration gradient is formed. If a gradient is still present, as judged by curvature of the fringes, a second redistribution is necessary.

Sedimentation Equilibrium Experiment. Several parameters have to be known in order to estimate: (1) the time required for the attainment of sedimentation equilibrium (Van Holde and Baldwin, 1958), (2) the gradient at the bottom of the solution, and (3) the time of overspeeding. The initial concentration (c_0) was measured from the experiment with the synthetic boundary cell, while r_m and r_b were predetermined by the manner in which the cell was to be filled. For these estimations, it is sufficient to know $M(1 - \bar{V}\rho_0)$ to about $\pm 15\%$. If not already known, it can be obtained from an Archibald experiment, an equilibrium experiment with a very short column of liquid (1 mm or less), or from the sedimentation coefficient of the material (see the discussion in Svedberg and Pedersen, 1940; Schachman, 1959).

The height that is chosen for the column of liquid depends upon the particular objectives of the experiment. Decreasing the height lessens substantially the duration of the experiment, but at the same time reduces both the accuracy of the molecular weight determination and the sensitivity to polydispersity. A column height of 3 mm proved a good compromise, giving molecular weights to an accuracy of about 1% or less for protein solutions at concentrations of

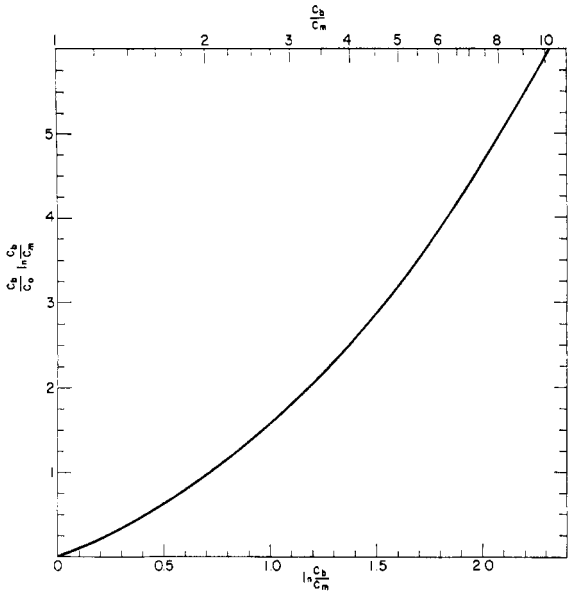

FIGURE 1: Determination of appropriate rotor velocity for sedimentation equilibrium.

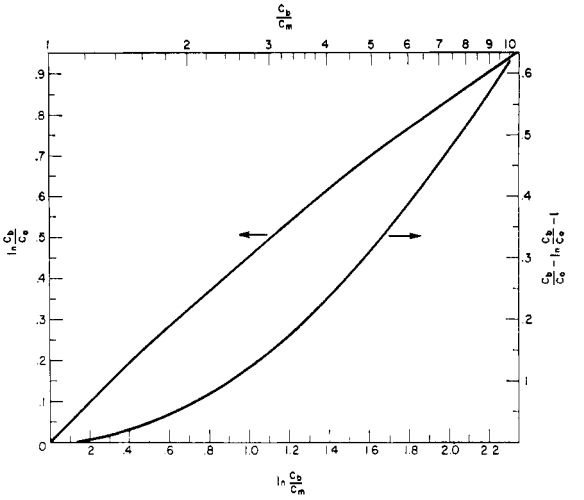

FIGURE 2: Determination of overspeeding time.

about 0.5 g/100 ml. For a 1-mm height, equilibrium is achieved in about one-tenth the time with an estimated error of about 3%.

Once the various parameters were known, the maximum velocity compatible with a reasonable value for $(dc/dr)_b$ was calculated. Even though it was found that 200 fringes/cm could be resolved, a value of 150 fringes/cm was used to leave room for a margin of error. A given set of conditions could be tested with eq 11 to see whether this value would be exceeded. It was found more convenient to plot $c_b/c_0 \ln c_b/c_m$ *vs.* $\ln c_b/c_m$ (see Figure 1; this plot was constructed by using convenient values for c_b/c_m, then calculating c_b/c_0 from eq 12). Then $\ln c_b/c_m$ was obtained graphically from the point which corresponded to the calculated value for $(dc/dr)_b(r_b^2 - r_m^2)/2c_0r_b$. The maximum velocity which could be used safely was then determined from eq 10.

If overspeeding was to be used, the necessary calculations were made with eq 17 by plotting $(c_b/c_0 - 1 - \ln c_b/c_0)$ and $\ln c_b/c_0$ *vs.* $\ln c_b/c_m$ (see Figure 2). With the estimated value for $\ln c_b/c_m$, obtained from eq 10, the overspeeding time was easily calculated. The optimum value of the angular velocity cannot be predicted from eq 17; but it should be neither so low that the plateau disappears during an appreciable part of the overspeeding period, nor so high that a highly concentrated layer of material is formed at the bottom of the solution. Experimentally it has been found that a close approximation of the equilibrium distribution was achieved sooner if the following sequence of speeds was used: (1) the rotor was held at a speed about 1.4 times the equilibrium speed for a period of time 10% longer than that calculated from eq 17 (during this time the plateau region disappears), (2) the rotor was rapidly decelerated to a speed of 0.7 times the equilibrium speed and held there for 5% of the time at the higher speed, and (3) the speed was brought back to that desired for the experiment and maintained for the duration of the centrifugation. The speed of the rotor was always reduced on fast brake, and increased at maximum amperage (this procedure did not lead to convective disturbances).

In order to plot $\ln c$ *vs.* r^2 the absolute concentration at various levels in the cell must be known. However, the intersection of the base line with the fringes on the equilibrium pattern locates only those positions which differ from the original concentration by integral numbers of fringes. Thus it is necessary to determine which of the intersections corresponds to the hinge point. After this is evaluated, the concentration at all levels can be calculated readily. The hinge point may be located by three different methods: (1) the utilization of the principle of the conservation of mass (Richards and Schachman, 1959), (2) the use of the white-light fringe to locate the hinge point (Richards and Schachman, 1959), and (3) the isolation of the hinge point on the pattern. The first method requires no preliminary preparation.

For the second method the refractive index of the reference liquid is increased to a value aprpoximating that of the solution by addition of another substance, which, to minimize redistribution, should have a low molecular weight and the same density as the solvent. This matching of the refractive indices of the two solutions improves the quality of the fringes since they are nearer the zero-order fringe. Thus the use of this technique is recommended for all low-speed experiments, except for those with high concentrations of low molecular weight additives (such as buffer salts or denaturants like urea). For this purpose 1,3-butanediol (Richards and Schachman, 1959) with a $\bar{V}$ of 0.981 ml/g (LaBar and Baldwin, 1962) proved ideal since its density is nearly the same as that of buffer solutions frequently used in studies on proteins. The addition of 0.10 ml of 1,3-butanediol to 10 ml of water or 0.2 M NaCl produces a refractive index increment equivalent to about 22 fringes. Higher densities can be obtained from the propanediol series or ethylene glycol, and intermediate values with suit-

able mixtures of these; for solutes dissolved in water, a better choice would be 1,5-pentanediol (Eastman) of density 0.994 g/cc, either used alone or mixed with 1,3-butanediol.

For the third method, the concentration change in the region of the hinge point must be followed almost continuously. This can be achieved by placing a narrow adjustable gate just before the photographic plate (Instruction Manual, Spinco Division, 1961) and taking 100 pictures or more at frequent intervals on a single plate. The experimental technique is described in the Instruction Manual, except that the gate should be positioned according to eq 18.

In general the use of a transparent immiscible liquid in the bottom of the cell is desirable, for it aids in the location of r_b and provides a sector-shaped interface. Three oils have been employed, fluorocarbon FC-43 (Yphantis, 1960), Kel-F no. 1 (Van Holde and Baldwin, 1958), and Dow Corning no. 555 silicone (Ginsburg *et al.*, 1956). The fluorocarbon was used routinely but if there were indications that this oil caused aggregation of the protein, a different oil (or no oil) was employed.

For most experiments the solution was overlapped by 0.005 ml of reference liquid at both centripetal and centrifugal ends to give interfaces that were distinct from those in the reference compartment. Usually 0.005 ml of oil and 0.11 ml of reference liquid were added to one compartment and the other was filled with 0.01 ml of oil and 0.10 ml of solution (which corresponded to a 3-mm column height). For solvent components that redistribute appreciably, the overlap should be avoided. An alternative procedure employed a double-sector centerpiece with communicating channels near the top and bottoms of the dividing rib. With this cell identical amounts of oil were added to both sides, but a slight excess (0.006–0.10 ml) of reference liquid was used. The equalization of hydrostatic pressure forced additional oil into the solution compartment, thereby providing a very small overlap at both ends.

If several determinations are to be made with the same material, or materials of nearly the same molecular weight, considerable time can be saved by examining two or more solutions simultaneously in a multicell rotor. Laterally wedged centerpieces, available commercially, permit the running of up to five solutions simultaneously. However, there are two drawbacks to this system: (1) the interfaces are not as distinct, and (2) the difference in optical path through the two compartments can lead to errors owing to redistribution of small components present in the solvent.

The six-channel cell of Yphantis (1964) permits the examination of three samples with appropriate reference liquids. The ease of filling the cell compartments should be weighed against the possibility of leakage from one compartment to another. Leakage between two solution compartments, or from solvent to solution compartment, is not important in high-speed sedimentation equilibrium (Yphantis, 1964), but is disastrous for the low-speed method. Moreover, the rectangular shape of the compartments requires a correction for the calculation of M_w^{app} and M_z^{app} from eq 4 and 8.

A system of masked upper window holders has been devised to permit the simultaneous examination of several solutions in a single experiment with separate ultracentrifuge cells for each sample (Teller, 1965). Since the maximum column height determines the number of cells that can be examined without overlapping of optical patterns, a different series of holders is needed for two-, three-, or four-cell operation. The window holder of each series was constructed with slots that permit light to pass through the desired portion of the radial opening of the centerpiece, the first slot allowing light to pass through the upper portion, the second, through the next portion, etc. These slots were so placed that there was an unexposed region between each image on the photograph. In Table I are shown the sizes of the slots and approximate values for the column heights. For higher speeds compression of the oil requires that its volume be increased slightly. An alternative method is to place masks made from shim stock between the upper window holder and the annular gasket used to support the window (R. Wade, personal communication). Oil was added to both compartments to a level just above the bottom of the slot. For double-sector centerpieces the volume in milliliters of liquid required to reach a given level (measured in centimeters from the center of rotation) is given by the approximate relationship, volume = $2.443 - 0.3393r$.

TABLE I: Specifications of Masked Window Holders for Multiple-Cell Operation.

No. of Cells	Slot Height (mm)	Max Column Height (mm)
2	6.4	5.9
3	4.4	3.9
4	2.5	2.0

If the white-light fringe method is to be used, the amount of 1,3-butanediol to be added is determined by counting the whole fringe number from the synthetic boundary experiment. The measurement was performed on the wet photographic plate to save time. Although the refractive index of the solution and the reference liquid need not be exactly the same, measurements are facilitated if they are within a few fringes of each other.

The cells filled in the desired manner were placed in the appropriate rotor with the unused holes in the four- or six-cell rotors occupied by appropriately balanced aluminum plugs. The rotor was accelerated to the chosen operating speed, and two interference pictures were taken immediately, one with the filter in place, and the other with white light. The rotor was then quickly brought to the speed selected for over-

speeding. Before it was time to reduce the speed, the first plate was developed and the time of overspeeding recalculated using the exact positions for the column extremities as measured on the wet plate. A white-light photograph was taken while a narrow region with nearly horizontal fringes still existed near the center of the cell (this is of use in locating the white-light fringe). After the rotor speed was reduced to the original value, pictures were taken at intervals until the equilibrium distribution was achieved.

Even though the equation of Van Holde and Baldwin (1958) provides a reliable estimate of the time required to reach equilibrium there is generally some hesitation about terminating an equilibrium experiment on the basis of this calculated time. Owing to the ever-present possibility of degradation or aggregation of the macromolecular solute during centrifugation, the only safe criterion for the attainment of equilibrium is that the concentration distribution no longer varies with time. Accordingly pictures were taken at intervals depending upon the molecular weight of the material. The attainment of equilibrium could then be ascertained by measuring the position of a few fringes near the cell extremities; when these values were constant the experiment was terminated.

Before the experiment is terminated both filtered and white-light interference pictures were taken. After the rotor had stopped the cell contents were mixed as described for the synthetic boundary experiment and another set of base-line patterns was obtained. This reexamination of the base-line pattern is especially important for experiments of long duration, because of the possibility of a change due to a shift in the cell windows, or to aggregation of the solute.

Evaluation of Interference Patterns. Since it is difficult to align interference patterns in the microcomparator and misalignment can lead to serious errors, we present here a procedure which permits rapid and accurate alignment of the photographic plates. The approach of Trautman (1956) was used to obtain directly from the photographs radial positions that are proportional to the radial distance in the cell from the axis of rotation. In the discussion to follow r is used to denote both these quantities, with the understanding that in the cell it is measured in centimeters and on the plate in millimeters. When it is necessary for the sake of clarity to distinguish between them, the dimension for the photograph is labeled with the additional subscript p. The dimension along the cross-motion of the stage, which is a measure of concentration, is given the symbol y.

The subscripts ir and or are used to denote the inner and outer reference edges of the counterbalance, and the subscript c refers to the position corresponding to $(r_{or} + r_{ir})/2$. In positioning the plate on the microcomparator r_c was used as the reference; this minimizes uncertainties in the position of the reference edges due to slight variations in the placement of the counterbalance as well as differences in the exposure and development of the photographs. Moreover, r_c is not influenced by variations in rotational placement of the counterbalance. Thus the plate was positioned with the reference edges centered about the scale reading corresponding to $10M_r r_c$, where M_r is the magnification factor in the radial direction. The value for r_c, assumed to be 6.50 cm, must be increased slightly at rotor velocities above 40,000 rpm (Schachman, 1959).

It is also possible to use the reference shadow on the plate produced by the wire that is built into the counterbalance cell. The position of this shadow is not affected by variations in exposure, but the quality is variable from one counterbalance to another. Moreover, the exact position of the wire is influenced by variations in rotational placement of the counterbalance.

If the Nikon microcomparator is used, it is desirable to make the inner reference edge appear to the left in the viewing screen; therefore the plate was inserted backwards, emulsion side up, in the holder. Alignment of the plate was simplified if the plate holder was adjusted until the inner reference edge was approximately centered in the stage opening. The distance between the reference edges was measured for the first pattern only. Thereafter each pattern was positioned initially so that the scale reading for the outer reference edge corresponded to $r_{or,p} = 10M_r r_c + (r_{or,p} - r_{ir,p})/2$. Then the stage was adjusted until the reference fringes produced by the counterbalance were parallel to the horizontal motion of the comparator. This was achieved by moving the stage to the left and holding it just to the left of the inner reference edge, adjusting the cross-motion until the central black fringe[2] was centered horizontally about the fiducial mark, and then returning the stage to the outer reference edge and rotating the goniometer until the central fringe was centered. This sequence was repeated until both reference hole patterns were centered about the fiducial mark. It was usually found that the outer reference edge had slightly shifted from the original setting for $r_{or,p}$. An adjustment can be made without touching the plate if provision for independent movement of the micrometer drum or its scale index is made. The Nikon Shadowgraph was equipped with zero-adjusting collars which permitted movement of the stage without changing the micrometer setting. Thus the collar was adjusted so that the micrometer read $r_{or,p}$ with the outer reference edge at the fiducial mark. The micrometer was then turned until the inner reference edge appeared beneath the fiducial mark. The micrometer reading was not necessarily the previously determined value $r_{ir,p} = 10M_r r_c - (r_{or,p} - r_{ir,p})/2$. To center the reference edges, the new reading for $r_{ir,p}$ and the calculated value were averaged. With the micrometer set at this number, the collar was adjusted to bring the inner reference edge to the fiducial mark. With this procedure meniscus values for patterns taken from the same

[2] No difficulty was experienced in locating the central fringe, since there is always an odd number of fringes in the reference holes, starting and ending with fringes of the same intensity. That there is an odd number of fringes is due to the fact that the central fringe is in the center of the diffraction envelope. The measurements were simplified by the installation of a bulls-eye (larger than the width of the fringes with four crossed lines separated by 45°) at the cross-hair.

TABLE II: Data Sheet for Synthetic Boundary Cell Experiment.[a]

Position in Cell	r (mm)[b]	Initial Pattern y (mm)	Resolved Pattern y (mm)	Base-Line Pattern y (mm)
1	36.5	0.843	0.903	0.578
2	37.0	0.840	0.902	0.575
3	38.0	0.836	0.895	0.567
4	51.0	0.992		0.557
5	52.0	1.000	1.060	0.562
6	53.0	1.004	1.071	0.566
		Fringe Shift		
6–1		0.161	0.168	−0.012
5–2		0.160	0.158	−0.013
4–3		0.156	c	−0.010
		Fringe Shift (corrected for base line)[d]		
6–1		0.173	0.180	
5–2		0.173	0.171	
4–3		0.166	c	
		0.171	0.175	

[a] Sucrose (1 g/dl) in H_2O, lateral fringe separation = 0.275 mm, whole fringe number = 31. The first pattern was taken immediately after superposition of the menisci; the second after resolution of the fringes in the boundary; the third after redistribution of cell contents. [b] Arbitrary values with r_{or} set at 57.19 mm. [c] This point lay within the boundary, so was not included. [d] Average concentration = 31 + (0.171/0.275) = 31.62 fringes.

experiment were reproducible to better than ±0.005 mm.

The procedure for the Gaertner microcomparator was similar, except that the plate was inserted frontwards, the holder adjusted to center approximately the outer reference edge in the stage opening, the cross-motion used to center the fringes in the outer reference hole, and the tangent screw turned to center the fringes in the inner reference hole. The nut holding the scale index was loosened so that small adjustments in readings could be made without movement of the stage.

Preliminary Examination of the Patterns. The determination of the weight-average molecular weight can be obtained by reading a minimum of five patterns: three from the synthetic boundary experiment and two from the equilibrium experiment. The complete evaluation of all the data available requires the examination of four more patterns from the latter. For the additional labor invested one obtains M_z^{app}, information concerning nonideality and/or heterogeneity, and increased confidence in the validity of the results.

Before considerable time was invested in a detailed reading of the patterns, several things were checked. The values for r_m and r_b from the beginning base line and the equilibrium patterns were compared to see whether a leak in the cell had occurred. For menisci that were not quite superimposed, the bottom portion of the interface shadow was used to give the values for the solution compartment. If there had been a leak in either sector the experiment was disregarded even though, in principle, corrections were possible.

The equilibrium base-line patterns taken at the beginning of the centrifugation and after redistribution of the cell contents were compared to confirm that there was no undue cell distortion or loss of solute. The white-light base lines were also checked, as it was possible to have had a shift of more than one fringe. Ordinarily it was found that the two base lines were nearly the same, but if there were a slight difference, the final pattern was chosen, since it was obtained closer in time to the equilibrium pattern. Three types of variation have been detected: a change in curvature, a lateral shift with no significant change in curvature, or both. A change in curvature was rare, whereas a small lateral shift, whether due to cell distortion, evaporation of water, or precipitation of protein, occurred frequently. However, a shift of less than 0.2 fringe is not usually experimentally significant, especially, where c_0 is 10 fringes or greater.

Determination of Initial Concentration from Synthetic Boundary Patterns. For the most accurate measurement of c_0 the whole number of fringes was determined from the pattern obtained after resolution of the boundary and the remaining fractional fringe from the pattern photographed just after superposition of the menisci. The base-line correction was made by using the pattern obtained after the redistribution of the cell contents. With this procedure it was possible to measure c_0 with an accuracy of ±0.01 fringe.

The pattern obtained after resolution of the boundary was aligned in the microcomparator, then the y values of a central fringe were determined for three to five positions of r near the meniscus at 0.5–1.0 mm intervals (see Table II). Without disturbing the cross-motion, the whole number of fringes across the boundary was counted, and the y values of the last fringe crossed were measured for three to five positions in the plateau region near the cell bottom. These same measurements were made for the pattern obtained just after superposition of the menisci, except that it was not usually possible to count the fringes across the boundary. The lateral fringe spacing was also determined by measuring the separation of five fringes near the meniscus. On the base-line pattern the y values of a central fringe were determined at the same positions of r.

To calculate the fractional fringe, the lateral separation of the outside, middle, and inside pairs of points was determined, then corrected for the corresponding shifts obtained from the base-line pattern. The final differences were divided by the fringe separation to obtain three to five determinations of the fractional fringe. (Occasionally a determination from the later pattern had to be discarded because a point was chosen within the boundary.) If no appreciable sedimentation occurred during the time interval between the two pictures the two sets of values agreed closely. When they differed it was usually possible to reconcile the

two by correcting for the movement of the boundary with the radial dilution equation. Generally the fractional fringe pattern was found to give the more reliable value.

Correction for Base-Line Distortion of Equilibrium Pattern. In the majority of experiments it was found that the fringes corresponding to the solution were not straight nor were they parallel to the reference fringes produced by the counterbalance. The shape and shift relative to the reference fringes varied with the speed of the rotor and was not necessarily constant in different experiments even when the same cell was used. Thus the beginning and final base line were determined routinely for every experiment by measuring the lateral displacement of the central fringe in the solution region relative to the central reference fringe.

After the pattern was aligned, the position y_{RF} of the central reference fringe was recorded. The stage was moved to locate the central fringe in the part of the pattern just to the right of the region of changing concentration near the meniscus. (This part of the pattern was usually displaced in the y direction, relative to the reference fringes.) This fringe was then followed across the cell, and the readings of r and y were noted. It was possible to reproduce readings of y to about ± 0.003 mm, which is equivalent to ± 0.01 fringe. The interval between readings depended upon the curvature; frequently it was found that 1- or even 2-mm intervals were sufficient. Finally the fringe separation was measured. The reading y_m near the meniscus was used as the zero point for the construction of a base-line plot, $y - y_m$ *vs.* r. The difference $y_m - y_{RF}$ was used to compare the two base lines, as well as to relate the base line to the equilibrium pattern.

The plot shown in Figure 3 is an example of the excellent agreement frequently obtained for the starting and final base lines. In this case a line representing an average was drawn. If the two patterns are grossly different, there is some uncertainty in the molecular weights obtained. For experiments in which it is suspected that material precipitated during the centrifugation, the starting base line is preferable.

If the regions of curved fringes near the extremities of the liquid column are too wide to permit extrapolation, they can be filled with data obtained from the subsequent centrifugation with the cell refilled with water (LaBar and Baldwin, 1962). Hopefully the water and solution base lines will exhibit the same curvature in the region where they overlap.

Measurement of Equilibrium Patterns. There are two methods for correcting for base-line distortion. The first involves reading the base line first, followed by incorporating the corrections as the equilibrium pattern is read. This procedure gives positions at constant fringe increments. The second method is to read fringe positions on the equilibrium pattern at a constant y value and then apply corrections for the base-line distortion by the appropriate calculations. The former is more laborious, but simplifies the calculations necessary for the conservation of mass. The latter is definitely the method of choice when a computer program is used to handle the data.

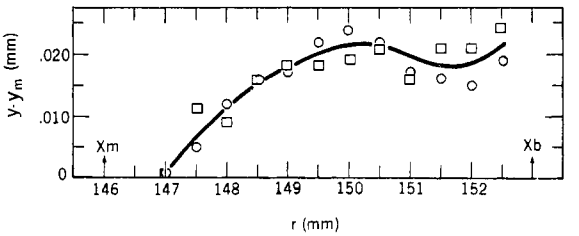

FIGURE 3: Base-line plot for sedimentation equilibrium (⊙) Beginning base line; (⊡) final base line. $r_{or} = 156.32$. $M = 2.1385$. $y_m - y_{RF}$ was 1.315 mm for the beginning base line and 1.309 mm for the final base line.

For the first method the pattern was aligned, y_{RF} was determined and added to $y_m - y_{RF}$ from the base-line pattern. The stage was moved from the meniscus to the cell bottom, following along the base line as provided by the addition of $y - y_m$ obtained from the base-line plot. As each fringe was crossed, its r position was carefully measured. The average of several readings gave values of r to about ± 0.005 mm. This procedure provided fringe positions at constant increments of one fringe, although, when desired, smaller or larger increments were used. For example, for half-fringe increments (useful when $c_b - c_m$ was small) the whole fringes were measured as above; then one-half the fringe separation was added to the value of y and the new fringe positions were noted. This procedure for measuring fractional fringes offers the possibility of greater accuracy than trusting the eye to locate in a consistent manner the centers of light and dark regions. The positions of r_m and r_b were also measured. A sample data sheet is shown in Table III.

For the second method, fringe positions were measured at the constant y value provided by the addition to y_{RF} of $y_m - y_{RF}$ from the base-line pattern. The appropriate y deflections from the base-line plot were converted to units of fringes, then subtracted from the concentrations as determined by the fringe number. For greater accuracy, the base-line pattern may be read at the r values corresponding to the fringe positions on the equilibrium pattern.

Location of Hinge Point. The position of the hinge point was determined by comparison of the white-light base-line pattern with the corresponding white-light pattern obtained at equilibrium. The stimulated intersection of the white-light fringes gave directly the radial position corresponding to the initial concentration. For identification purposes, the central of the three relatively clear, black fringes was employed, although identical results were obtained with either of the other two (as long as they were properly matched in the two patterns). With the base-line pattern aligned in the microcomparator, the "y" distance was measured between the white-light fringe in the reference holes and the corresponding fringe at a position about 0.55 of the distance through the solution column (eq 18). After alignment of the equilibrium pattern, the cross-motion in the y direction was set to the same distance above the fringes in the reference holes. The position

TABLE III: Data Sheet and Calculations for Conservation of Mass.[a]

y^b (mm)	$y^{1}/_{2}{}^c$ (mm)	Fringe No.	r^d (mm)	c^e (fringes)	c^f (fringes)	Log c^g	r^2 (cm^2)
		Meniscus	145.966	27.60	27.66	1.4419	46.590
0.839		1	146.627	28.23	28.29	1.4516	47.013
	0.981	2	147.150	28.73	28.79	1.4592	47.349
0.847		3	147.706	29.23	29.29	1.4667	47.707
	0.993	4	148.220	29.73	29.79	1.4741	48.040
0.856		5	148.715	30.23	30.29	1.4813	48.361
	0.999	6	149.236	30.73	30.79	1.4884	48.700
0.860		7	149.712	31.23	31.29	1.4954	49.012
	1.003	8	150.220	31.73	31.79	1.5023	49.345
0.860		9	150.665	32.23	32.29	1.5091	49.638
	0.999	10	151.145	32.73	32.79	1.5157	49.954
0.857		11	151.575	33.23	33.29	1.5223	50.237
	1.001	12	152.018	33.73	33.79	1.5288	50.533
0.860		13	152.478	34.23	34.29	1.5352	50.839
		Bottom	153.125	34.93	34.99	1.5402	51.272

$$c_1 - c_m = \frac{r_1 - r_m}{r_2 - r_1}(c_2 - c_1) = \frac{146.627 - 145.966}{147.150 - 146.627}(0.5) = 0.63 \text{ fringe}$$

$$c_b - c_N = \frac{r_b - r_N}{r_N - r_{N-1}}(c_N - c_{N-1}) = \frac{153.125 - 152.478}{152.478 - 152.018}(0.5) = 0.70 \text{ fringe}$$

$$c_b - c_m = (c_1 - c_m) + c_N - c_1 + (c_b - c_N) = 0.63 + 6.00 + 0.70 = 7.33 \text{ fringes}$$

$$r_b^2 - r_m^2 = 51.272 - 46.590 = 4.682 \text{ cm}^2$$

$$\int_{c_m}^{c_b} r^2 dc = \Delta c(r_1^2/2 + \sum_{2}^{N-1} r_1^2 + r_N^2/2) + (c_1 - c_m)(r_1^2 + r_m^2)/2 + (c_b - c_N)(r_b^2 + r_N^2)/2 = (0.5)(587.803) +$$
$$(0.63)(47.013 + 46.590)/2 + (0.70)(51.272 + 50.839)/2 = 359.126 \text{ fringes-cm}^2$$

$$c_0 - c_m = \frac{r_b^2(c_b - c_m) - \int_{c_m}^{c_b} r^2 dc}{r_b^2 - r_m^2} = \frac{(51.272)(7.33) - 359.126}{4.682} = 3.57 \text{ fringes}$$

$$M_w^{app} = \frac{1}{A} \frac{c_b - c_m}{c_0(r_b^2 - r_m^2)} = \frac{(6.6656 \times 10^{-3})(7.33)}{(31.23)(4.682)} = 334.1$$

[a] A 1% solution of sucrose was sedimented for 275 min at 42,040 rpm. Temperature, 25°; c_0, 31.23; $1/M$, 0.46762; $1/A$, 6.6656×10^3; $r_b - r_m$, 3.35 mm. Fringe 7 corresponds to the hinge point. [b] The difference $y_m - y_{RF}$ from the base-line pattern was added to y_{RF} for the equilibrium pattern; then $(y - y_m)$ from the base-line plot was added. [c] One-half the fringe separation (0.142 mm) was added to y_{RF}. Then the additions were performed as in the previous column. [d] The average of at least three readings. [e] Fringe 7 was labeled with the value of c_0, 31.25 fringes; the other values were obtained by adding increments of 0.50 fringe. c_m was obtained from $c_1 - (c_1 - c_m)$ and c_b, from $c_N + (c_b - c_N)$. [f] These values were obtained by subtracting $c_0 - c_m$ from c_0 to find c_m, adding $c_1 - c_m$ to find c_1, adding Δc to find other concentrations, and adding $c_b - c_N$ to find c_b. [g] Log of values in column 6.

obtained by adjusting the horizontal motion until the white-light fringe in the solution was centered about the fiducial mark was the hinge point. A sample data sheet is shown in Table IV. Comparison of the position of the white-light fringe with fringe positions obtained with monochromatic light shows that the hinge point corresponded to the fringe at 129.911 mm. (It should be noted that a monochromatic fringe corresponds to the white-light fringe even though the values of $y - y_{RF}$ were not the same.) Owing to blurring of the pattern obtained with polychromatic light, a difference in 0.03 mm for the positions of the white-light fringe and the corresponding monochromatic fringe is not significant. In some cases it was difficult

TABLE IV: Location of Hinge Point from White-Light Fringe.[a]

Pattern	y_{RF} (mm)	y_r (mm)	$y - y_{RF}$ (mm)	r (mm)
White-light base line	19.614	19.990[b]	0.276	
		$y - y_{RF}$	y_r	
White-light equilibrium	19.593	0.276	19.869	129.89
Monochromatic equilibrium	18.895	0.086	18.981[c]	129.422
		0.087	18.982	129.663
		0.088	18.983	129.911
		0.092	18.987	130.142
		0.094	18.989	130.365

[a] Patterns from an experiment with RNase. [b] Measured at about 0.55 of the distance from r_m to r_b. [c] Obtained from base-line plot as described in text.

to decide which of several clear, black fringes was the white-light fringe; this identification was aided by examination of the white-light pattern taken during the overspeeding period. If the white-light fringe was not visible in the base-line pattern, another characteristic fringe was used instead.

Location of r_b. The greatest source of error in M_w^{app} and M_z^{app} stems from the uncertainty in the determination of c_b and $(d \ln c/dr^2)_b$ due in part to the inability to locate r_b precisely. The uncertainty can be as much as several per cent, since the concentration changes most rapidly in this region. At equilibrium the steep concentration gradient near the bottom of the column solution causes the light to bend into the oil interface, where at least a part of it is reflected. This effect is enhanced by the presence of aggregated or denatured material, most of which ends up at or near the interface. The combination of both strongly deviated and reflected light produces a region on both schlieren and interference patterns that is difficult to interpret. There is even a point at which the fringes appear to be discontinuous, bending sharply downward. To help in the location of r_b on the equilibrium pattern one can use the base-line pattern at the beginning of centrifugation as an aid. (The final base line is more difficult to read if any aggregated or denatured material forms during the centrifugation). Even very early in the centrifugation the bottom interface is somewhat complicated, but at this stage the uncertainty is considerably less. The value for r_b on the equilibrium pattern can be estimated by adding to r_m the value $(r_b - r_m)$ evaluated from the base-line pattern.

One way of improving the accuracy in locating the interface positions would be to fill the cell reproducibly with a micrometer syringe. To correct for effects arising from refractive index gradients, a preliminary calibration can be performed with the correct volumes of oil and water added to the cell. Since the location of the interfaces is influenced by the orientation of the cell in the rotor, it should be oriented so as to have the same relative position of the scribe lines on cell and rotor, as examined with the aid of a low power (8–10×) ocular. Pictures should be taken at the speed chosen for the equilibrium speed. Comparison of interface shadows on calibration and equilibrium patterns would improve the accuracy in the location of r_m and r_b.

Calculations

Manual. Molecular weights were calculated most readily through the use of eq 4 since this requires the evaluation of $c_b - c_m$, but not fringe positions; c_0 is obtained from the experiment with the synthetic boundary cell. An appropriate correction was made if the centerpieces used for the synthetic boundary and equilibrium experiment differ in thickness. Since the fringe pattern does not extend to the extremities of the solution column, an extrapolation was required. The concentration difference from the meniscus to the first fringe was approximated by

$$c_1 - c_m = \frac{r_1 - r_m}{r_2 - r_1}(c_2 - c_1) \tag{19a}$$

and from the last fringe (N) to the bottom

$$c_b - c_N = \frac{r_b - r_N}{r_N - r_{N-1}}(c_N - c_{N-1}) \tag{19b}$$

Thus

$$c_b - c_m = (c_1 - c_m) + c_N - c_1 + (c_b - c_N) \tag{20}$$

To construct a plot of ln c *vs.* r^2 it was necessary to find the concentration at one point; the concentration at other points was obtained by adding or subtracting fringe increments. The concentration difference between the hinge point and the meniscus was found from the expression for the conservation of mass

$$c_0 - c_m = \frac{r_b^2(c_b - c_m) - \int_{c_m}^{c_b} r^2 dc}{r_b^2 - r_m^2} \tag{21}$$

The integral term was evaluated by the trapezoidal rule, with a linear extrapolation to the extremities of the column (see Table III)

$$\int_{c_m}^{c_b} r^2 dc = \Delta c(r_1^2/2 + \sum_{2}^{N-1} r_i^2 + r_N^2/2) + (c_1 - c_m)(r_1^2 + r_m^2)/2 + (c_b - c_N)(r_b^2 + r_N^2)/2 \tag{22}$$

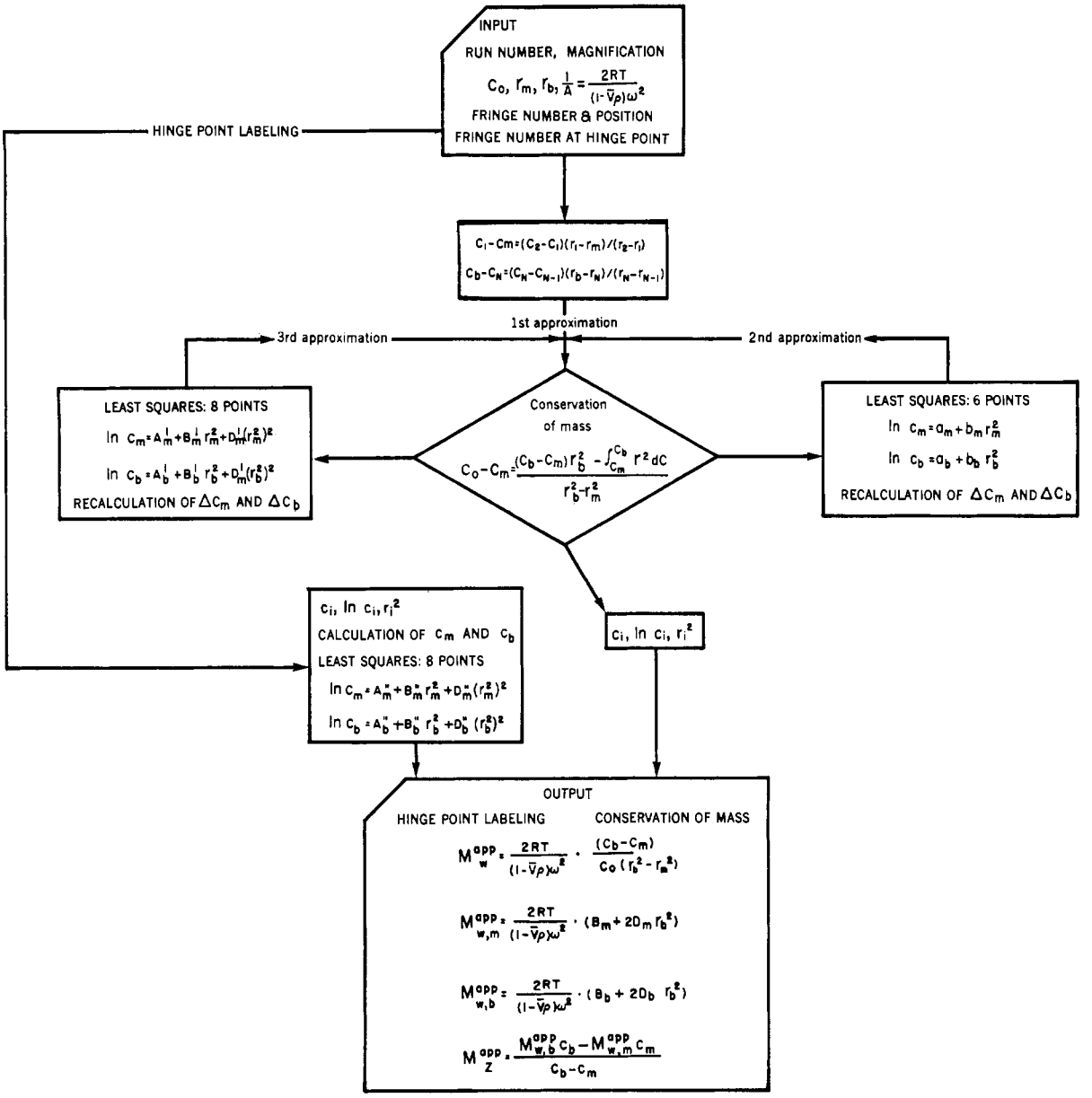

FIGURE 4: Block diagram of computer program with hinge-point labeling and three approximations for conservation of mass.

where Δc is the fringe increment, usually a single fringe.

From eq 21 and c_0, c_m was calculated; then ($c_1 - c_m$) was added to find c_1 and fringe increments were added to find the concentrations at other points. From the nearly linear plot of ln c *vs.* r^2, c_b and c_m were determined with greater accuracy by extrapolation and the resulting value inserted again into eq 21 and 22 to produce a more reliable value of $c_0 - c_m$. If this value was significantly different from the former one, a new ln c *vs.* r^2 plot was constructed. Additional extrapolations to r_m and r_b, if necessary, were performed by fitting an appropriate number of points with a least-squares linear or quadratic equation. Note that for eq 20 and 22, only $c_1 - c_m$ and $c_b - c_N$ assume new values after each approximation. Finally $c_b - c_m$ was used to find M_w^{app} and the slope at the extremities to find M_z^{app} from eq 8.

The value obtained for $c_0 - c_m$ can be used to locate which of the fringe positions corresponds to c_0, since they were measured in a manner such that they correspond to concentrations that differ from c_0 by integral numbers of fringes. The labeling is accomplished by "adding" fringes to $c_0 - c_m$ until a value near c_0 is reached. This fringe position is assigned the value c_0, and the other fringes are labeled in the manner already described. This method can be used as a check for the location of the white-light fringe without going to the trouble of assigning concentrations on the basis of the value for $c_0 - c_m$ obtained from conservation of mass.

Use was made of the hinge point as determined from

the white-light pattern by assigning the value for c_0 to the position r_0, and the concentrations at the other points were determined by adding or subtracting integral numbers of fringes. The value for $c_b - c_m$ was obtained from the plot of ln c *vs.* r^2 extrapolated to the interfaces and M_z^{app} from the slopes at the extremities.

The calculations necessary to find $c_0 - c_m$ are shown at the bottom of Table III. The values of c in the fifth and sixth columns were obtained from hinge-point labeling and from conservation of mass, respectively. The value for $c_0 - c_m$ was 3.57 from the first approximation of conservation of mass, 3.54 from a quadratic fit of eight points at the meniscus and bottom of the log c *vs.* r^2 plot, and 3.63 from hinge-point labeling. The calculated value for M_w^{app} was 334.1 for the first approximation, compared to 335.9 from the quadratic fit.

Computer Program Involving Mass Conservation and Hinge-Point Labeling. In order to increase the accuracy and decrease the tedium of computations from sedimentation equilibrium data, a computer program was developed for hinge-point labeling and mass conservation calculations (Teller, 1965). A block diagram illustrating its basic features is shown in Figure 4. Allowances are made for calculations with or without the white-light fringe, and for the use of fractional or whole fringe intervals in plate reading. The conservation of mass treatment consists of three approximations to the hinge point, essentially as described previously for manual computation: (1) the use of eq 19a, (2) a least-squares linear fit of the first and last six points, and (3) for inhomogeneous or nonideal systems a least-squares quadratic fit over the points in the top and bottom third of the cell, using at least eight points. After each determination of $c_b - c_m$, the values of c are recalculated before the next extrapolation. For hinge-point labeling the calculated concentrations are used to extrapolate to the cell extremities according to the quadratic extrapolation procedure just described.

Separate output is obtained for conservation of mass and hinge-point labeling. Besides M_w^{app}, M_z^{app}, $M_{w,b}^{app}$, $M_{w,m}^{app}$, and $M_{w,c}^{app}$, tables are constructed for c, ln c, the deviation of ln c from the least-squares straight line through all the points (useful for locating "bad" points due presumably to plate reading errors), and the deviation of ln c from the least-squares straight line joining ln c_m and ln c_b (useful for detecting curvature). Also included is the value of $M_{w,r}^{app}$ at each point obtained by a least-squares cubic fit of groups of nine points.

Computer Program for Fitting ln c vs. r^2 Data. Frequently for computer analyses of data from sedimentation equilibrium experiments, it is advantageous to have a single equation which represents the concentration distribution throughout the entire cell. Such an equation is also useful for "smoothing" of random errors arising from reading of the interference patterns. Since ln c is a linear function of r^2 for an ideal, two-component system and samples often are contaminated with higher molecular weight aggregates, it is reasonable to fit ln c with a power series in r^2 according to

$$\ln c = \sum_{i=0}^{n} a_i r^{2i}$$

To evaluate the number of terms necessary to fit the data adequately, a computer program was developed to handle from two to six terms. As starting data, it uses the output from the previous program together with the necessary constants. It then calculates the desired least-squares curves to fit the points, as well as the deviations of the calculated values of ln c. Finally M_w^{app}, $M_{w,m}^{app}$, $M_{w,b}^{app}$, $M_{w,c}^{app}$, and M_z^{app} are found from the derivatives of the above equation.

Results and Discussion

Concentration Measurement with the Synthetic Boundary Cell. Since the value of c_0 required for calculating M_w^{app} from eq 4 is usually obtained from an experiment with a double-sector synthetic boundary cell, it is important to evaluate the accuracy of such measurements. The performance and reliability of the cell were tested by determining the number of fringes (J) obtained from a solution containing a solute of known concentration and specific refractive increment (dn/dc) and comparing it with the value calculated from the expression

$$J = \frac{ac\dfrac{dn}{dc}}{\lambda} \qquad (23)$$

where a is the thickness in the direction of the optical path and λ is the wavelength of the light used.

Preliminary experiments with sucrose solutions gave low values for the measured number of fringes (about 0.5% less than expected). In view of this finding, various tests were made to evaluate the performance of the cells and to eliminate possible sources of error.

To test for adsorption of solute on the cell walls a series of three measurements were made using the same sucrose solution. In the first, the cell parts were subjected to the usual drying procedure; in the second, the centerpiece was dried in a desiccator over P_2O_5; in the third, the solution compartment was rinsed several times with the sucrose solution before being filled. The number of fringes obtained were, respectively, 31.63, 31.62, and 31.64, demonstrating that the low values for the number of fringes were not due to the adsorption of solute to the cell walls. The excellent agreement among the three values shows the precision of such measurements.

The possibility of convection during the layering process was investigated by adding adenosine to either the upper or the lower layer and looking for its presence in the other region in the cell with the ultraviolet absorption system. For these experiments a normal double-sector cell (as used with the schlieren optical system) was assembled with a mask in the upper window

TABLE V: Validity of Synthetic Boundary Cell.[a]

Soln	Concn (g/dl)	J, Fringes: Measured	J, Fringes: Calcd[b]	J/c, Fringe-dl/g
1	1.0026_6	31.28	31.36	31.20
2	2.0021_1	62.50	62.62	31.22
3	2.5023_3	78.13	78.27	31.22
4	3.0073_3	93.83	94.07	31.20
5	4.0061_1	125.03	125.53	31.20
			Av	31.21
			Eq 23	31.28[b]

[a] A stock sucrose solution was diluted gravimetrically. The concentration of the resulting solutions was measured at 25° using the same synthetic boundary cell. For solutions 4 and 5 the whole fringe number was assumed. [b] Calculated from $dn/dc = 1.430 \times 10^{-3}$ dl/g, $\lambda = 5.463 \times 10^{-5}$ cm, $a = 1.195$ cm.

holder to prevent the passage of light through the solvent limb. In one experiment water was layered over a solution containing 10 mg/ml of sucrose and 1.8 mg/ml of adenosine (absorbance of about 100). If allowance was made for an error of 0.5 cm in the height of the densitometer tracing (10 cm corresponded approximately to an absorbance of 1), it is estimated that less than 0.05% dilution of the upper layer occurred. When adenosine at 3.6 mg/ml was layered over a 15-mg/ml sucrose solution there was less than a 0.02% dilution of the lower layer. Thus convection can be eliminated as an explanation for the low fringe measurements.

Finally, attention was focused on the three variables (dn/dc, a, and λ) in eq 23. For sucrose dn/dc at 25° is reported to be 1.430×10^{-3} dl/g (Gosting and Morris, 1949). This value was confirmed by making measurements of the number of fringes observed for solutions of sucrose of known concentration in a Spinco Model H electrophoresis–diffusion apparatus. Careful measurements on the assembled cell showed that, upon tightening, the centerpiece thickness decreased about 0.7% from 12.04 to 11.95 mm. The transmission maximum of the Baird–Atomic B-9 filter was found to be 546.3 mμ. When these values were combined to calculate the expected number of fringes from a sucrose solution of known concentration, the value, though much closer to that expected, was still 0.2% low. The results of several such experiments always gave a value about 0.2% lower than expected. A summary of results with solutions of sucrose is presented in Table V.

It seems likely that the low value for the measured number of fringes is due to an incorrect value for λ and, to a lesser extent, for a. Since the 546.1-mμ line of mercury is known to be broadened by the high pressure in the AH-6 lamp, the effective wavelength of the light passing through the filter and exposing the photographic plate is difficult to determine. Also the exact value for the centerpiece thickness to be used for the rotating cell is uncertain owing to the possibility of distortion. (The effect of rotor velocity on centerpiece thickness could be evaluated by counting the fringes for a boundary at different speeds.)

Since a more accurate determination of a and λ is extremely difficult, a given synthetic boundary cell was calibrated with a solution containing a solute of known concentration and specific refractive increment and the constant a/λ evaluated by combining these values with the experimentally determined value of J. With this constant one can determine the concentration of other solutes if dn/dc is known. In order to illustrate this approach the various results for sucrose solutions (Table V) have been rearranged in column 5 to give J/c. The internal consistency for J/c provides an excellent demonstration of the reproducibility of synthetic boundary measurements. From the average value of J/c and dn/dc one finds a/λ to be 2.182×10^4 compared with 2.197×10^4 if nominal values of 1.2 cm for a and 546.1 mμ for λ are assumed. If, instead of the nominal cell thickness, the measured value after compression is employed the agreement is much better. It should be emphasized that the value for a/λ must be checked for other combinations of light filters, light sources, and centerpieces.

Evaluation of Computer Program with Simulated Data. To test the computer program, error-free data representing different types of systems were desired. In addition the effect of experimental errors on the conservation of mass calculations had to be assessed. Consequently an additional computer program was developed to simulate various experimental situations with both perfect and imperfect data. For this program the input contained the initial concentration, molecuar weight, and partial specific volume of the solute as well as the relevant "experimental" factors, such as the positions of the meniscus and cell bottom, the rotor speed, and the magnification of the optical system. In addition the program simulated experimental data for heterogeneous systems by stipulating the weight fractions of a specific number of components of given molecular weight. To simulate reading error a feature which permitted the introduction of a chosen random error in fringe position was incorporated into the program. The program produced for each system the expected fringe positions at constant increments of one fringe, one of which was the hinge point. In addition it gave the concentration and the number- and weight-average molecular weights for each fringe position in the cell. Near the bottom of the cell, fringe positions of separation less than 0.06 mm were discarded. This was done to simulate the experimental situation in which closely spaced fringes near the bottom of the cell cannot be resolved.

Sets of data obtained for a variety of hypothetical systems were treated with the conservation of mass computer program. The results are shown in Table VI. For a two-component system (trial 1), chosen to represent a 3.1-mm column of a 0.5% ribonuclease solution at a speed to give c_b/c_m of about 3, the molec-

TABLE VI: Computer Treatment of Simulated Data.[a]

Trial	Std Error (mm)	Components		$M_{r,\bar{c}}^{app}$	M_w^{app}			M_z^{app}		
		M	Wt Fraction		In	Out	Error (%)	In	Out	Error (%)
1	0	13,243	1	13,243	13,243	13,243	0	13,243	13,255	0.09
2	0.005	13,070	1	13,136	13,070	13,057	0.10	13,070	13,173	0.79
3	0	13,070	0.99	13,197	13,201	13,196	0.04	13,330	13,284	0.35
		26,140	0.01							
4	0.005	13,243	0.9	20,673	25,159	17,548	30	75,949	26,035	66
		132,400	0.1							
		13,000	0.366							
		26,000	0.400							
5	0.005	39,000	0.160	25,963	25,376	24,678	2.7	31,168	27,660	11.3
		52,000	0.064							
		65,000	0.010							

[a] $c_0 = 18.55$ fringes, $r_b - r_m = 3.1$ mm, $A^{-1} = 4.995 \times 10^4$.

TABLE VII: Effect of Reading Error on Molecular Weights from Conservation of Mass.[a]

Variation	Std Dev (mm)	M_w (Av)	Std Dev (%)	M_z (Av)	Std Dev (%)
All points except r_m and r_b	0	13,243		13,254	
	0.005	13,240	0.1	13,247	0.7
	0.010	13,235	0.2	13,243	1.0
	0.020	13,237	0.3	13,154	2.0
r_b and r_m only	0.015	13,239	0.2	13,254	0.1

[a] Starting data obtained from trial 1, Table VI.

ular weight results were accurate to better than 0.1%. There were no significant differences in the results from the conservation of mass treatment or that based on hinge-point labeling. The extrapolated values for c_b and c_m were correct to 0.004 fringe. The small error in M_z^{app} arose from slight errors in interpolation procedures employed in the program. When a 0.005-mm standard error was incorporated into the fringe position (trial 2) M_w^{app} was still accurate to 0.1% while the error in M_z^{app} increased to 0.8%.

Trial 3 represents a mixture containing 1% dimer, with no experimental error. The extrapolation to find c_b and c_m with the small curvature present in the ln c *vs.* r^2 plot presented no problem for the program. However, the computer program could not handle an unlikely mixture containing 10% of a material of ten times higher molecular weight (trial 4). Because of the extreme accumulation of the heavier material near the bottom of the cell, the extrapolation gave 6.6 instead of 18.4 fringes for $c_b - c_N$. For trial 5, representing a hypothetical interacting system containing monomer through pentamer, the extrapolation to the cell bottom gave $c_b - c_N$ of 9.2 fringes, close to the correct value of 10.3 fringes. This error resulted in an error of only 2.7% in M_w.

To investigate further the effect of errors in locating fringe positions the perfect data in trial 1 of Table VI was used to obtain thirty different sets of fringe positions, ten each with standard deviations of 0.5, 0.10, and 0.020 mm. The only restrictions imposed were that deviations greater than three standard deviations were excluded, and the values for r_m and r_b were left unchanged. The average values of M_w^{app} and M_z^{app} for the 30 sets of data run through the conservation of mass program are shown in Table VII. Also included in the table are molecular weights with r_m and r_b randomized nine times with standard deviation of 0.015 mm and the correct values for the other fringe positions. In all cases randomization had little effect.

With careful reading of interference patterns, including the averaging of several values for each fringe position, the standard deviation is about 0.005 mm. This error in the experimental data should lead to an estimated accuracy of about 0.2% for M_w^{app} and about

TABLE VIII: Comparison of Hinge-Point Labeling and Conservation of Mass.[a]

Material	c_0	c_m		$c_b - c_m$		M_w^{app}		M_z^{app}	
		CM[b]	HP[c]	CM	HP	CM	HP	CM	HP
Sucrose	31.23	27.690	27.630	7.367	7.368	335.9	335.9	323.1	323.1
	46.73	41.841	41.685	10.074	10.074	336.1	366.1	289.0	289.0
RNase	28.37	16.362	16.397	28.941	28.941	13,243	13,243	14,012	14,011
	14.04	5.683	5.484	22.885	22.885	13,226	13,225	14,198	14,203
	7.11	2.318	2.385	14.153	14.154	13,227	13,227	14,223	14,219

[a] The results were obtained from the conservation of mass computer program. Concentrations are units of fringes. [b] Conservation of mass treatment. [c] Labeling of hinge points.

1% for M_z^{app}. For less careful readings with a standard deviation of 0.015 mm, the accuracy should be better than 0.5% for M_w^{app} and 2% for M_z^{app}.

For a plot of ln c *vs.* r^2 with upward curvature the question arises as to what slope represents the average for the polydisperse solute. Clearly, some position in the cell has the correct average, even though it may not have the same distribution of the various species. This position is also a function of the velocity at which the experiment is performed. As a check on the determination of M_w^{app} from eq 4 it is suggested that the slope of ln c *vs.* r^2 at the position corresponding to $(c_b + c_m)/2$ be used. Examination of values for $M_{w,\bar{c}}^{app}$ shown in Table VI reveals that molecular weights determined at this position are reasonably close to the weight-average molecular weights even for the rather extreme cases considered in trials 4 and 5.

Hinge-Point Labeling. A comparison of the results obtained from hinge-point fringe labeling and from conservation of mass treatment was made in order to assess the reliability of the two methods. In Table VIII are shown results from the computer treatment of data obtained from equilibrium experiments with sucrose and with RNase. For nearly all experiments the difference in c_m calculated by the two methods was less than 0.20 fringe and on the average it was about 0.10 fringe. It should be noted that even for the RNase experiment with a difference of 0.20 fringe or the sucrose experiment with a difference of 0.06 fringe, the two methods yielded results that were virtually identical (to four decimal places). This excellent agreement generates confidence that (1) all the material in the cell was accounted for, (2) the fringe labeling was correct, and (3) no arithmetic errors were made in the calculations.

Sedimentation Equilibrium of 1,3-Butanediol. The redistribution of 1,3-butanediol was verified experimentally by centrifuging a 7-mm solution at an initial concentration of 100 fringes (about 5% concentration) at 52,640 rpm. Under these conditions the concentration difference from top to bottom was 1.49 fringes. From eq 4, $\bar{V}$ was found to be 0.975 ml/g, close to the value of 0.981 ml/g obtained by LaBar and Baldwin (1962), who used a density gradient column. This small difference could arise from effects of nonideality or convection in the sedimentation equilibrium experiment. However, if corrections for these were to be included, the value for the partial specific volume would be shifted even lower. The difference could also be due to the fact that our sample was not redistilled, or that 1,3-butanediol is compressible. For the moment, the origin of the discrepancy in partial specific volume of 1,3-butanediol as determined by the two methods remains unclear.

Whenever it is necessary to correct for the redistribution of small components present only in the reference liquid, it is preferable to use the value of $M(1 - \bar{V}\rho_0)$ as determined from a sedimentation equilibrium experiment. The conditions should be as close as possible to those employed for the solution under investigation. Thus the buffer should be placed in the compartment usually reserved for the solution, with the reference liquid in its usual place.

Sedimentation Equilibrium of Sucrose. Sucrose was chosen as the primary test material for sedimentation equilibrium because of its homogeneity and the availability of thermodynamic data describing the nonideality of solutions as a function of concentration (Gosting and Morris, 1949). A series of solutions ranging from 1 to 4 g/dl was prepared; three cells with column heights of about 3.3 mm were run simultaneously using the masked window holders described earlier. 1,3-Butanediol was added to the reference liquid for only two experiments at 3 and 4 g/dl. (Experiments were also performed at these concentrations with only H_2O in the reference cell; although the patterns could be read, the fringes were less distinct and greater difficulty was experienced in making the measurements.) With our value for $\bar{V}$, correction was made for the sedimentation of 1,3-butanediol; it was assumed that the hinge point was located at $(r_m + r_b)/2$. (The use of 0.981 rather than 0.975 ml/g reduces M_w^{app} by 0.4%.)

The data from these experiments were treated by the computer program, using both the method of conservation of mass and that of hinge-point labeling. For the experiments in which 1,3-butanediol was not added, the fringe position corresponding to the hinge point was chosen on the basis of close agreement of

TABLE IX: Comparison of Least-Squares Curve Fitting with Conservation of Mass for Sucrose.[a]

Treatment	n[b]	Av Dev ($\times 10^4$)[c]	$M_{w,m}^{app}$	$M_{w,b}^{app}$	M_w^{app}	M_z^{app}
Least squares	2	5.3			329.5	
	3	3.3	338.0	321.1	329.2	256.6
	4	2.8	344.4	327.6	330.1	264.8
Conservation of mass			344.3	324.7	330.0	250.1

[a] $c_0 = 2.502$ g/dl, $c_b - c_m = 18.14$ fringes. [b] The number of terms used to fit ln c as a power series in r^2. [c] Average deviation in ln c, experimental values and least-squares curve.

c_m obtained from the conservation of mass and hinge-point treatments. As the two treatments yielded the same results to four significant figures only data obtained for conservation of mass are reported here. The values for ln c and r^2 were also treated by the least-squares computer program which fits the points to a power series

$$\sum_0^n a_i (r^2)^n$$

where n may vary from 1 to 5. (The advantage of this program is that all the points may be used for the determination of c_m and c_b as well as for the calculation of the apparent molecular weights at r_m, r_b, and $r_{\bar{c}}$). In all cases the ln c *vs.* r^2 data were adequately represented by a cubic equation, as determined by the fact that the average deviation did not decrease for higher values of n. Comparison of results from the least-squares treatment and the conservation of mass treatment are shown in Table IX. Three findings are particularly noteworthy: (1) the nearly constant value of $c_b - c_m$ (as reflected in M_w^{app}) for the three-curve fittings and the eight-point quadratic extrapolation at both extremities used in the conservation of mass; (2) the rather close agreement for $M_{w,m}^{app}$, $M_{w,b}^{app}$, and $M_{w,\bar{c}}^{app}$; and (3) the rather poor, but consistent, values obtained for M_z^{app}.

In Figures 5 and 6 are shown results obtained from the conservation of mass program, as well as those from the least-squares cubic fit of all the points. Examination of the plots shows that there is no essential difference in results obtained by the two methods. For example, the least-squares straight line through the points in Figure 5A (conservation of mass) is

$$\frac{1}{M_w^{app}} = 2.904 \times 10^{-3} + 5.27 \times 10^{-5} c$$

and through the points in Figure 5B

$$\frac{1}{M_w^{app}} = 2.908 \times 10^{-3} + 5.21 \times 10^{-5} c$$

where c is measured in grams per deciliter.

The activity data for sucrose quoted by Gosting and Morris (1949) can be represented by the equation

$$\ln y = 1.044 \times 10^{-2} c + 0.725 \times 10^{-4} c^2$$

With the calculated values for B_1^*, and B_2^*, and the molecular weight (342.30), the concentration dependence for the molecular weight of sucrose can be expressed as

$$\frac{1}{M_w^{app}} = 2.9214 \times 10^{-3} + 4.855 \times 10^{-5} c + 7.24 \times 10^{-7} c^2$$

Values of $1/M_w^{app}$ were calculated for the concentrations used in the experiments. The least-squares straight line through these points is

$$\frac{1}{M_w^{app}} = 2.9178 \times 10^{-3} + 5.21 \times 10^{-5} c$$

In view of the short columns and rather low concentrations that were used, the agreement of the slope (5.27×10^{-5} *vs.* 5.21×10^{-5}) and the extrapolated molecular weights (344.3 *vs.* 342.7) is excellent.

For the other plots in Figures 5 and 6 the dotted line indicates the expected plot on the basis of the activity data. It should be noted that for Figure 5C,D the points fall close to the expected line, indicating the values for $M_{w,\bar{c}}^{app}$ are very good. The better agreement of the molecular weight values at $r_{\bar{c}}$ compared to those at r_m and r_b is due to the fact that interpolation is inherently more accurate than extrapolation. In Figure 6A,B, where the ordinate has been contracted, the points obtained from data at the meniscus generally fall below the theoretical line, while the values evaluated from the bottom of the liquid column are in better agreement. This means that the slope at the meniscus is higher than expected. The higher values obtained for the molecular weight at the meniscus are reflected in the wide divergence of the points for $1/M_z^{app}$ in Figure 5C. Owing to the small change in slope of the ln c *vs.* r^2 plot a small error in the molecular weights at r_m and r_b produces a larger effect in M_z^{app}. Why

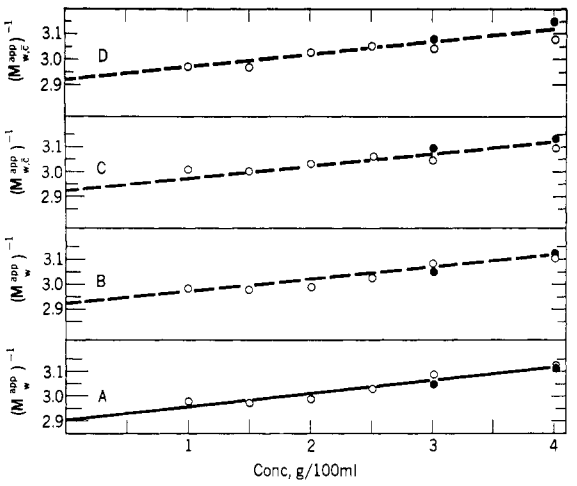

FIGURE 5: Molecular weight of sucrose. The apparent molecular weights are plotted against $(c_b + c_m)/2$. The shaded points refer to experiments for which 1,3-butanediol was added to the reference liquid. (A and C) Results from conservation of mass computer program. (B and D) Treatment of results from conservation of mass computer program with least-squares computer program. Solid line: least-squares straight line through the points. Dashed line: line calculated from known molecular weight and second virial coefficient obtained from isopiestic data.

consistently low values were obtained for the molecular weight at the meniscus remains unclear; in the first experiment the cells were centrifuged for the time required (4 hr) to reduce the error in M_w^{app} to 0.002, and in the other two experiments even longer periods were employed (Van Holde and Baldwin, 1958).

In summary, the results obtained from sucrose solutions show that the determination of M_w^{app} and $M_{w,c}^{app}$ is reliable. However, if curvature in ln c *vs.* r^2 plots is small, values of M_z^{app} are uncertain.

Sedimentation Equilibrium of Ribonuclease. When it had been demonstrated that satisfactory results could be obtained with a substance of low molecular weight, the investigation of a homogeneous protein was undertaken. RNase was chosen as a test material because of its known chemical purity. Since the sample had not been freeze dried after chromatographic purification it should have been free of dimers (Yphantis, 1960, 1964).

The RNase solution at about 7 mg/ml was dialyzed for 2 days at 0° against buffer (0.1 M NaCl–0.01 M ethanolamine, pH 9.5) near its isoelectric point. After the synthetic boundary experiment (day 1) the sedimentation velocity patterns (day 2) obtained with Rayleigh optics were examined to see if all of the sedimenting material could be accounted for. Then dilutions of the stock RNase solution were made gravimetrically with the final buffer used for dialysis to give five additional solutions with concentrations ranging down to 2 mg/ml, numbered in order of decreasing concentration. Three sedimentation equilibrium experiments in separate cells with masked window holders were performed simultaneously. The three

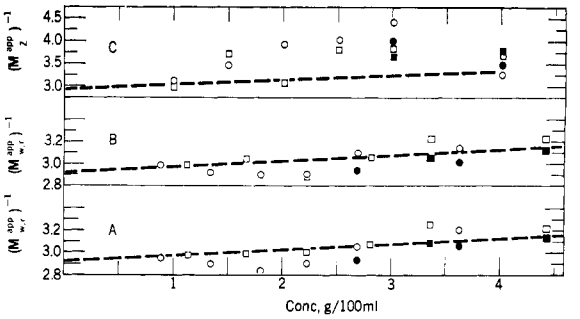

FIGURE 6: Molecular weight of sucrose. Results are from same experiments as shown in Figure 5; A and circles of C correspond to 5A,C; B and squares of C correspond to 5B,D. (A and B) Circles, molecular weights of meniscus; squares, molecular weights at bottom. Other notation same as Figure 5.

most concentrated solutions were run first (day 3), positioned in the cells in order of decreasing concentration from the center of rotation. The velocity was selected so that the maximum gradient for resolvable fringes at the bottom of the solution column would be achieved in one cell, but not exceeded in the others. At the conclusion of the first run, the second series of three solutions was centrifuged at a higher velocity selected in the same manner (day 5). Finally, as a check on the gravimetric dilutions, the concentrations of the second, third, and sixth solutions were determined with the synthetic boundary cell (day 6).

Analysis of the interferograms from the synthetic boundary experiments revealed that the measured fringe numbers did not correspond to the dilutions determined gravimetrically. Thus the concentrations of solutions 2, 3, and 6 calculated from the stock solution were lower than the measured value by about one fringe. This error could most easily be explained either by contamination of the buffer with water after the performance of the first synthetic boundary experiment or by evaporation of water from the diluted RNase solutions.

Analysis of interferograms from the sedimentation velocity experiment was made difficult by the fact that by the time the meniscus region was clear of protein, the plateau region was lost. By superposition of suitable patterns and corrections for base-line distortion and radial dilution, the concentration of the stock solution was found to be 28.76 fringes, compared to 28.34 fringes measured from the synthetic boundary experiment. A fractional fringe number of 0.42 fringe was obtained by comparison of fringes in the meniscus region on patterns taken at the beginning of centrifugation and after the protein had sedimented. The three values for the fractional fringe were in reasonably close agreement, indicating that the material measured in the synthetic boundary cell was of sufficient molecular weight to sediment away from the meniscus. Also there did not appear to be any large material that sedimented in a short period of time.

Because of the discrepancies in the results of the synthetic boundary experiments, the molecular weight

TABLE X: Sedimentation Equilibrium of RNase.[a]

Soln	c_0 Fringes	$c_b - c_m$ Fringes	$M_{w,m}^{app}$ ($\times 10^{-4}$)	$M_{w,b}^{app}$ ($\times 10^{-4}$)	M_z^{app} ($\times 10^{-4}$)	$M_{r,c}^{app}$ ($\times 10^{-4}$)	M_w^{app} ($\times 10^{-4}$)
1[b]	28.37	28.87	1.316	1.324	1.328	1.325	1.321
2[b]	24.16	27.24	1.317	1.328	1.334	1.334	1.327
3[b]	18.46	21.05	1.338	1.317	1.307	1.315	1.316
4[c]	14.04	22.78	1.252	1.332	1.352	1.324	1.316
5[c]	10.80	21.31	1.264	1.324	1.334	1.321	1.311
6[c]	7.11	14.03	1.239	1.327	1.342	1.325	1.311
					Av 1.333 ± 0.014		1.317 ± 0.08

[a] Solvent: 0.1 M NaCl–0.01 M ethanolamine (pH 9.5). Column height, 3.2 mm; rotor, four cell (AN-F); temperature, 25°; 1,3-butanediol added to reference liquid. [b] Centrifuged 27 hr (including overspeeding) at 17,250 rpm. [c] Centrifuged 10 hr (including overspeeding) at 21,740 rpm.

determinations were suspect and ordinarily would have been discarded. In spite of uncertainties in the validity of the results, the experiments are useful here for illustrating (1) the internal consistency of data obtained in low-speed equilibrium experiments, (2) the effect of errors in c_0 on curvature of ln c *vs.* r^2 plots, and (3) the pitfalls that can arise upon incomplete evaluation of available data.

The data from the equilibrium experiments were treated with the conservation of mass computer programs. The value of c_0 determined from the synthetic boundary experiment was used for the stock solution; for the others, values were calculated from the gravimetric dilution factors. Again, the results obtained from hinge-point labeling and from conservation of mass were comparable. The latter are included in Table X. In column 2 are shown the initial concentrations in fringes. The values for $c_b - c_m$ are also given, because they are a direct measure of the precision of M_w^{app}. If effects of nonideality are ignored, the precision in M_w^{app}, $M_{w,c}^{app}$, and M_z^{app} is excellent. Comparison of the average values for M_w^{app} and M_z^{app} would suggest that the material exhibited but little heterogeneity, as evidenced by the slightly higher values for the latter. Further examination revealed that the values of $M_{w,m}^{app}$ for the three most dilute solutions, run at a higher speed so that heterogeneity was more evident, were lower than those for $M_{w,b}^{app}$. In fact, the values at the meniscus were much lower than the value of 13,680 calculated on the basis of the amino acid composition (Hirs *et al.*, 1956). If the higher values for c_0 determined with the synthetic boundary cell were used, the discrepancy became even greater. Correction of the concentrations for having focused half-way rather than two-thirds through the cell (Svensson, 1954) produced no significant change in either the calculated molecular weights or in the curvature of the ln c *vs.* r^2 plots.

In order to evaluate the curvature in the ln c *vs.* r^2 plots in terms of possible heterogeneity in the protein preparation, the points were fitted with power series by means of the least-squares program. The adequacy of the curve fitting was about the same for each set of data; the results from one set are shown in Table XI. It was found that M_w^{app} was essentially independent of the number of terms used to fit the points, indicating that the last four equations for ln c as a function of r^2 gave essentially the same concentrations at the column extremities. However, there was greater variation in the extrapolated values, $M_{w,m}^{app}$ and $M_{w,b}^{app}$, and therefore in M_z^{app}.

Decreasing the values for c_0 in each experiment reduced the curvature in the ln c *vs.* r^2 plots and improved the agreement between the various calculated molecular weights and the accepted value. To investigate the effect of a variation in c_0 on the conservation of mass program, it was assumed that there was an unknown amount of material that did not redistribute in the centrifugal field. An algebraic analysis of the series expansion of d ln c/dr^2 for a two-component mixture was used to find the amount of a hypothetical contaminant of "zero" molecular weight that would give rise to the r^4 term determined from curve fitting. Then the calculated amounts of contaminant were used to

TABLE XI: Comparison of Least-Squares Curve Fitting with Conservation of Mass Treatment.[a]

Constants[b]	$M_{w,m}^{app}$ ($\times 10^{-4}$)	$M_{w,b}^{app}$ ($\times 10^{-4}$)	M_z^{app} ($\times 10^{-4}$)	M_w^{app} ($\times 10^{-4}$)
2	1.304	1.304	1.304	1.304
3	1.247	1.355	1.372	1.317
4	1.227	1.338	1.356	1.313
5	1.227	1.337	1.356	1.313
6	1.281	1.379	1.395	1.316
Conservation of mass	1.239	1.327	1.342	1.311

[a] Curve fitting for solution 6 of Table X. [b] Number of terms used to fit ln c as a power series in r^2.

TABLE XII: Effect of Small Change in c_0 on Conservation of Mass Results.[a]

Soln	Δc_0 Fringe	$M_{w,m}^{app}$ ($\times 10^{-4}$)	$M_{w,b}^{app}$ ($\times 10^{-4}$)	M_z^{app} ($\times 10^{-4}$)	M_w^{app} ($\times 10^{-4}$)	$(M_{calcd}^{app})^b$ ($\times 10^{-4}$)
1	−0.28	1.334	1.334	1.334	1.334	1.337
2	−0.23	1.356	1.338	1.329	1.341	1.341
4	−0.53	1.374	1.366	1.365	1.369	1.350
5	−0.24	1.347	1.343	1.342	1.341	1.354
6	−0.28	1.395	1.361	1.356	1.367	1.358

[a] Same starting data as used for Table X, except that c_0 was changed by amount noted in column 2. Solution 3 was omitted because curvature in ln c *vs.* r^2 was a very small, negative number. [b] Calculated from $M^{app} = M/(1 + 0.03c)$. Concentrations calculated assuming $dn/dc = 0.00187$ dl/g, $a(dn/dc)/\lambda = 40.9$.

correct the values of c_0, and the equilibrium data were treated again with the conservation of mass program. The new values for the molecular weights, together with the calculated amounts for the contaminant (Δc_0 in column 2), are shown in Table XII. Also included in the table for purposes of comparison are the apparent molecular weights calculated on the basis of an assumed value of 0.03 dl/g for the second virial coefficient. The small changes in c_0 improved considerably the agreement among the various molecular weights calculated for a single experiment. Moreover, the values for M_w^{app} are much closer to the accepted molecular weight (13,680), and to the estimated apparent molecular weights listed in the last column.

It should be emphasized that such "tampering" with experimental data, though instructive, may be misleading. For example, the curvature in ln c *vs.* r^2 plots may, in fact, be due to heterogeneity. It was done here only to show how small errors in c_0 can lead to a different interpretation of the results. The inconsistencies in c_0 found for this series of experiments have not been observed for other samples.

Effect of Overspeeding. In order to evaluate the effectiveness of overspeeding, two equilibrium experiments were performed, one at constant velocity and the other with the sequence of speeds described in the Experimental Section. When overspeeding is employed it is not sufficient to use invariance of the fringe positions near the cell extremities as a criterion for the attainment of equilibrium since it is possible to have a nearly constant value for $c_b - c_m$ while the concentrations within the liquid column have not attained the equilibrium values. Thus, for an evaluation of the attainment of the equilibrium distribution, the fringe positions for the entire pattern were treated with the conservation of mass computer program; the results are shown in Table XIII. For the moment we will consider only the values of M_w^{app}.

TABLE XIII: Overspeeding and Time to Equilibrium.[a]

Time (hr)	M_w^{app} ($\times 10^{-4}$)	$M_{w,m}^{app}$ ($\times 10^{-4}$)	$M_{w,b}^{app}$ ($\times 10^{-4}$)	M_z^{app} ($\times 10^{-4}$)
		Constant Velocity		
3.2	1.247	1.246	1.596	1.722
5.3	1.378	1.320	1.533	1.595
6.4	1.416	1.405	1.555	1.597
11.8	1.449	1.315	1.624	1.707
13.9	1.432	1.343	1.489	1.529
17.7	1.430	1.347	1.489	1.527
		Overspeeding[b]		
1.3	1.442	1.667	1.362	1.280
1.3	1.450	1.658	1.462	1.410
1.6	1.402	1.426	1.436	1.439
2.2	1.403	1.364	1.527	1.573
4.3	1.408	1.364	1.485	1.519
5.3	1.411	1.308	1.526	1.587
6.4	1.420	1.347	1.563	1.623
7.5	1.418	1.337	1.531	1.585
10.0	1.422	1.361	1.567	1.624

[a] RNase (Armour) at 0.5 g/dl; $r_b - r_m$, 2.82 mm; T, 25°; velocity, 20,410 rpm; $c_b - c_m$, approximately 28 fringes; c_0, 18.41 fringes; ln (c_b/c_m), 1.50. [b] Centrifuged for 68 min at 29,500 rpm, 3 min at 14,290, then at 20,410 rpm for duration of experiment. The times noted were measured from the moment the rotor *first* reached 20,410 rpm.

In the experiment at constant velocity, the equilibrium distribution was achieved between 6.4 and 11.8 hr. According to the equation of Van Holde and Baldwin (1958), the distribution at 7.3, 9.3, and 11.1 hr should yield values of $c_b - c_m$ that differ from the equilibrium value by 1.0, 0.3, and 0.1%, respectively.

With the overspeeding sequence described earlier the distribution at 2.2 hr was very close to that at 7.5 or 10 hr; at 4.3 hr it was indistinguishable. Thus a substantial reduction in time, similar to that obtained by Hexner *et al.* (1961), was achieved.

It is interesting to compare the overspeeding time calculated from eq 17 with that obtained from the plots of Hexner *et al.* (1961). Under the conditions of the experiment the calculated times are, respectively, 62 min compared to 65 min.

The initial decision to overspeed at 1.4 times the equilibrium velocity (Richards, 1960) was arbitrary; no other ratios were investigated. The plots of Hexner *et al.* (1961) include a continuum of overspeeding velocities, but no attempt was made to show which one gave the shortest time to achieve equilibrium.

Since the effect of overspeeding at a variety of speeds was not investigated, it is not possible to state which method would give the greatest reduction in time. Both methods involve assumptions and approximations; hence it is difficult to predict which is preferable. Further documentation, both theoretical and experimental, is required before the final choice can be made. Moreover, more exacting criteria for the attainment of equilibrium, including evaluation of molecular weights at the column extremities, should be explored. It is likely that several speed changes will produce the equilibrium distribution even sooner.

Errors in c_0. It is clear that any error made in c_0 leads to an error in M_w^{app}. If dialysis of the material under investigation has not been complete, the resulting salt gradient in the synthetic boundary centrifugation will give rise to an incorrect value for c_0. In this case, or if dialysis is for some reason impossible, c_0 can still be determined accurately, but more laboriously, from a normal velocity centrifugation using the interference optical system (Richards and Schachman, 1959).

Strictly speaking the base-line level used to represent c_0 for the equilibrium pattern cannot be used as an absolute measure of c_0. Its lateral position, relative to the central fringe in the reference holes, is influenced by three variables: (1) uneven compression of the centerpiece, (2) failure to add the exact amount of 1,3-butanediol required to raise the refractive index of the reference liquid to that of the solution, and (3) a gradient of small, nonsedimenting molecules arising from failure to achieve dialysis equilibrium. None of these influence the position of the hinge point, whether determined from conservation of mass or from use of the white-light fringe. However, correct labeling of the hinge point requires that c_0 as measured in the synthetic boundary experiment be correct.

An interesting case arises if, during a long experiment, part of the material aggregates and sediments to form a thin pellet at the bottom of the column. The white-light fringe method still locates the position in the cell at which the concentration is equal to the initial value (c_0) measured from the synthetic boundary experiment. Therefore, the plot of ln c *vs.* r^2 (based upon the white-light fringe) remains valid for the determination of M_z^{app}. But the use of eq 4 to calculate M_w^{app} is not correct, since the measured value for c_0 does not represent the correct concentration of the material to be used with the value of $c_b - c_m$. However, the value which should be used for c_0 can be obtained from the position on the concentration curve (white-light data) which corresponds to the hinge point as determined with the values of $c_0 - c_m$ obtained from the conservation of mass.

Thus, the two methods for the location of the hinge point serve to complement each other and both should be used if at all possible. If they give the same value for c_m within experimental error (about 0.2 fringe), this is good evidence that r_m and r_b were accurately located and that no material was lost from the solution during the equilibrium experiment.

Final Evaluation. It has been shown that patterns from synthetic boundary experiments on solutions of about 1 g/100 ml and equilibrium experiments on 3-mm columns of solutions of concentration greater than 0.2 g/100 ml can give molecular weights to an accuracy of 0.5% or greater. This accuracy was realized with sucrose, but not with the particular RNase sample used in the work reported here. In spite of the high precision obtainable with low-speed sedimentation equilibrium, it is a common occurrence that the sample under investigation is not sufficiently homogeneous to give plots of ln c *vs.* r^2 that are straight or curved downward (nonideality). It is interesting to mention here that, in a study involving low-speed sedimentation equilibrium of purified chicken myosin, a plot $1/M_z^{app}$ *vs.* c had about twice the slope of that for $1/M_w^{app}$, in agreement with eq 3 and 9; moreover, the close agreement of the molecular weights extrapolated to zero concentration was consistent with the sample being but slightly contaminated with aggregates (Richards *et al.*, 1967).

The potential accuracy of the low-speed method can be attained more easily than that with the high-speed method (Yphantis, 1964) for two reasons: (1) measurements are made over the total length of the column; (2) errors in fringe positions at the higher concentrations are less significant. Moreover, in the high-speed method, data obtained near the meniscus, where concentrations are very low, are often uncertain. Errors in concentration can also arise from optical aberrations that are greatest near the cell bottom (Svensson, 1954). Since these errors are proportional to the square of the refractive index gradient, which is about the same for both kinds of experiments, they are more serious with the lower concentrations that are employed in the high-speed method. (For a more detailed discussion of these errors, the reader is referred to Yphantis, 1964.)

However, the greater accuracy with the low-speed method is obtained at the cost of more labor, an additional centrifuge run, and more patterns to be read. Whether the additional labor is warranted depends upon the objectives of the worker. Clearly, for very dilute solutions obtained from chromatography experiments, the method of Yphantis is the only choice with interference optics. But when sufficient material is available, it is desirable to do both determinations for a more complete characterization. The high-speed method is less sensitive to higher molecular weight contaminants, but very sensitive to smaller contaminants. When it is desired to study interacting systems, it may be necessary to use higher concentrations that are not suitable with the high-speed method.

It is clear that the accuracy of the low-speed method depends upon the accuracy with which the initial concentration is determined from the synthetic boundary experiment. Thus, it is recommended that this measurement be made routinely several times. Moreover, a careful determination is of little use if the material has

not reached dialysis equilibrium. In spite of the great accuracy of the synthetic boundary determination, the worker should be aware of the danger of convection at concentrations lower than about 3 mg/ml. Finally, it should be emphasized that a sedimentation velocity experiment on the most concentrated solution is useful to demonstrate that all of the material in the cell is accounted for, and that no unusually large or small material is present in the sample.

A complete evaluation of newer techniques introduced in low-speed equilibrium has not been made. To enable the use of longer columns of solution, improved methods are needed to reach equilibrium sooner. The theoretical treatment of Hexner *et al.* (1961) should be extended to include several speed changes. There has recently been developed a special cell which permits the layering of four different solutions, thereby producing an immediate step-function approximation to the final equilibrium distribution (Griffith, 1967). At the conclusion of the experiment, the contents are mixed, the reference compartment is rinsed and filled to the top with solvent, and a synthetic boundary experiment performed to find c_0. The performance of an equilibrium and synthetic boundary experiment in the same cell had already been described by Boeyé (1965).

The method of LaBar (1965) of increasing the speed at the end of the equilibrium experiment to find the zero reference level on the interferogram needs further work to assess its accuracy. The method is difficult to apply to solutions of concentrations higher than a few milligrams per milliliters. The interesting possibility of combining interference and schlieren data (Richards and Schachman, 1959; Chervenka, 1966) may be worth further investigation.

In conclusion, it is interesting to consider whether improvements in the automatic split-beam photoelectric scanner, with its ability to handle such low concentrations that nearly all solutions become ideal, will eliminate the need for the Rayleigh interference optical system (Schachman and Edelstein, 1966; Edelstein and Schachman, 1967). Conceptually this method is the one of choice, since absolute concentrations are determined directly and therefore no additional experiment or treatment is required to provide a reference, either for high- or low-speed sedimentation equilibrium experiments. Another advantage of the scanner is that the presence of small contaminants cannot be overlooked, as is possible with the high-speed experiments of Yphantis (1964). However, the scanner is limited to materials which absorb light in some region of the spectrum and to nonabsorbing solvent systems. Finally, it should be pointed out that there are systems which can be profitably investigated through the simultaneous use of the absorption and Rayleigh optical systems, as, for example, the interaction between bovine plasma albumin and methyl orange (Steinberg and Schachman, 1966).

References

Beams, J. W., Snidow, N., Robeson, A., and Dixon, III H. M., (1954), *Rev. Sci. Instrum. 25*, 295.

Billick, I. H., Dishon, M., Schulz, M., Weiss, G. H., and Yphantis, D. A. (1966), *Proc. Nat. Acad. Sci. U. S. 56*, 399.

Boeyé, A. (1965), *Virology 25*, 550.

Chervenka, C. H. (1966), *Anal. Chem. 38*, 356.

Donnelly, T. H. (1966), *J. Phys. Chem. 70*, 1862.

Edelstein, S. J., and Schachman, H. K. (1967), *J. Biol. Chem. 242*, 306.

Fujita, H. (1962), Mathematical Theory of Sedimentation Analysis, New York, N. Y., Academic.

Fujita, H., and Williams, J. W. (1966), *J. Phys. Chem. 70*, 309.

Ginsburg, A., Appel, P., and Schachman, H. K. (1956), *Arch. Biochem. Biophys. 65*, 545.

Goldberg, R. J. (1953), *J. Phys. Chem. 57*, 194.

Gosting, L. J., and Morris, M. S. (1949), *J. Am. Chem. Soc. 71*, 1998.

Griffith, O. M. (1967), *Anal. Biochem. 19*, 243.

Gropper, L. (1964), *Anal. Biochem. 7*, 401.

Hexner, P. E., Radford, L. E., and Beams, J. W. (1961), *Proc. Nat. Acad. Sci. U. S. 47*, 1850.

Hirs, C. H. W., Moore, S., and Stein, W. H. (1956), *J. Biol. Chem. 219*, 623.

Klenin, S. T., Fujita, H., and Albright, D. A. (1966), *J. Phys. Chem. 70*, 946.

LaBar, F. E. (1965), *Proc. Nat. Acad. Sci. U. S. 54*, 31.

LaBar, F. E. (1966), *Biochemistry 5*, 2368.

LaBar, F. E., and Baldwin, R. L. (1962), *J. Phys. Chem. 66*, 1952.

Lansing, W. D., and Kraemer, E. O. (1935), *J. Am. Chem. Soc. 57*, 1369.

Mason, M., and Weaver, W. (1924), *Phys. Rev. 23*, 412.

Osterhoudt, H. W., and Williams, J. W. (1965), *J. Phys. Chem. 69*, 1050.

Richards, E. G. (1960), Doctoral Dissertation, Department of Biochemistry, University of California, Berkeley, Calif.

Richards, E. G., Chung, C.-S., Menzel, O. G., and Olcott, H. S. (1967), *Biochemistry 6*, 528.

Richards, E. G., and Schachman, H. K. (1959), *J. Phys. Chem. 63*, 1578.

Schachman, H. K. (1959), Ultracentrifugation in Biochemistry, New York, N. Y., Academic.

Schachman, H. K., and Edelstein, S. J. (1966), *Biochemistry 5*, 2681.

Steinberg, I. Z., and Schachman, H. K. (1966), *Biochemistry 5*, 3728.

Svedberg, T. (1925), *Kolloid Z. 36*, 53.

Svedberg, T., and Pedersen, K. O. (1940), The Ultracentrifuge, New York, N. Y., Oxford University.

Svensson, H. (1950), *Acta Chem. Scand. 4*, 399.

Svensson, H. (1954), *Opt. Acta 1*, 25.

Teller, D. C. (1965), Doctoral Dissertation, Department of Biochemistry, University of California, Berkeley, Calif.

Trautman, R. (1956), *J. Phys. Chem. 60*, 1211.

Van Holde, K. E., and Baldwin, R. L. (1958), *J. Phys. Chem. 62*, 734.

Williams, J. W., Van Holde, K. E., Baldwin, R. L., and Fujita, H. (1958), *Chem. Rev. 58*, 715.

Yphantis, D. A. (1960), *Ann. N. Y. Acad. Sci. 88*, 586.

Yphantis, D. A. (1964), *Biochemistry 3*, 297.